SUPPLEMENTARY INFORMATION FOR "Synthesis and patterning of tunable multiscale materials with engineered cells"

Allen Y. Chen, Zhengtao Deng, Amanda N. Billings, Urartu O.S. Seker, Michelle Y. Lu, Robert J. Citorik, Bijan Zakeri, Timothy K. Lu

Supplementary Figures

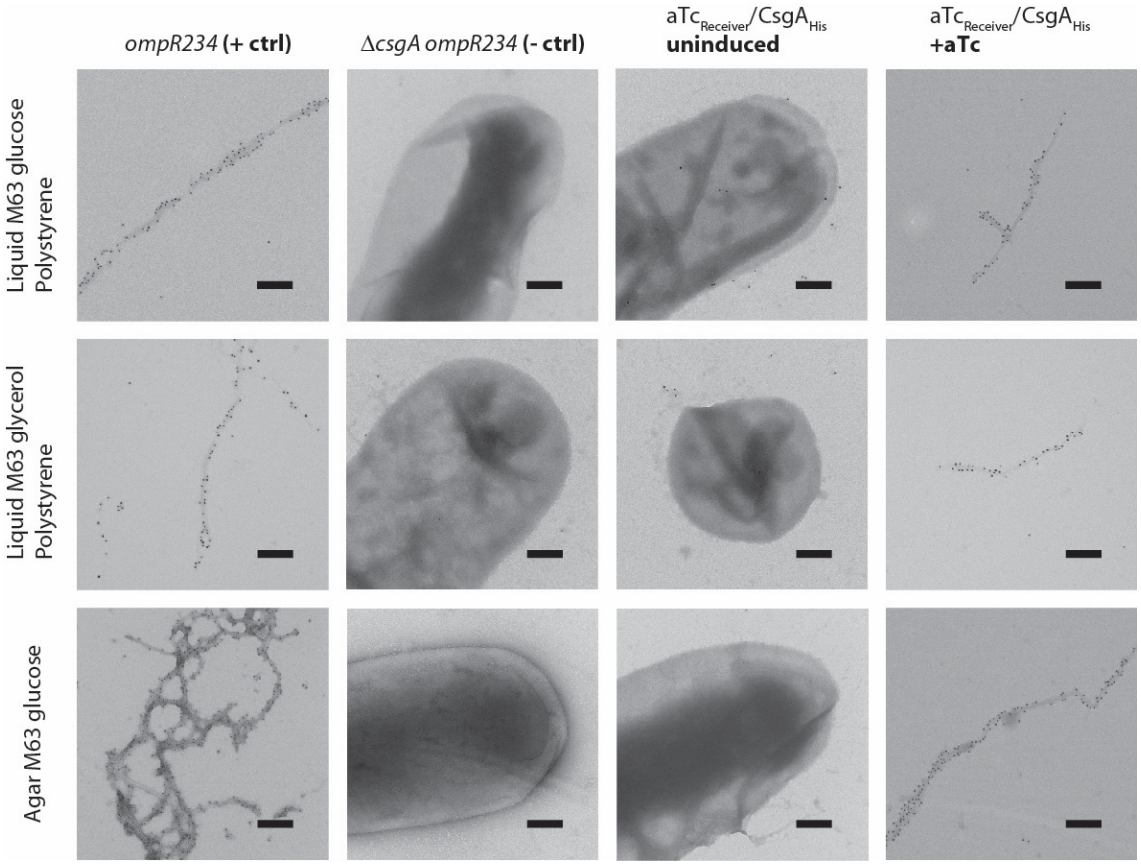

Supplementary Figure 1 | Immuno-labelling of curli fibrils with rabbit anti-CsgA antibodies and gold-conjugated goat anti-rabbit antibodies. This data shows that *E. coli* MG1655 *ompR234* cells ("*ompR234*", see Supplementary Table 3), which have an intact endogenous *csgA* gene, produce curli fibrils that are labelled by anti-CsgA antibodies and attached to cells. However, cells with the *csgA* gene knocked out and no *csgA*-expressing circuits ("Δ*csgA ompR234*", see Supplementary Table 3), and aTc$_{Receiver}$/CsgA$_{His}$ cells in the absence of aTc, did not produce curli fibrils. Inducing aTc$_{Receiver}$/CsgA$_{His}$ cells with aTc enabled the production of curli fibrils that were labelled by anti-CsgA antibodies and attached to cells. This was the case for all culture conditions used (see Supplementary Methods): liquid M63

with glucose on Thermanox (Fig. 1b), liquid M63 with glucose on polystyrene, liquid M63 with glycerol on polystyrene, and M63 with glucose in 0.7% agar. Scale bars are 200nm.

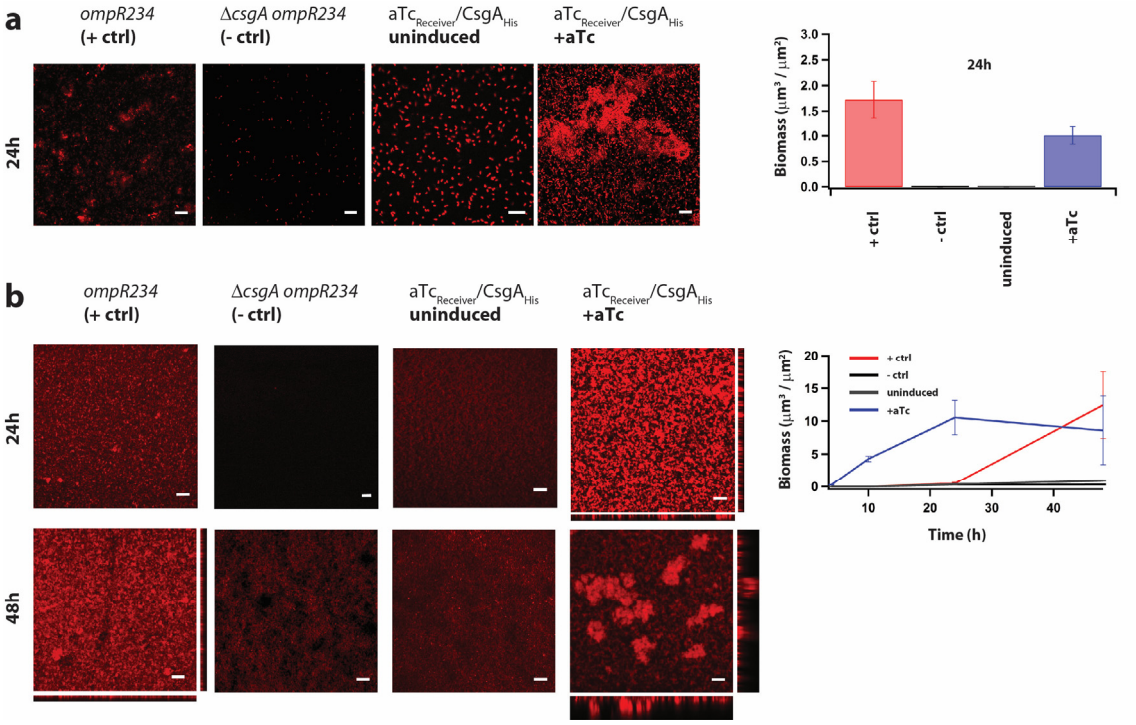

Supplementary Figure 2 | a, Confocal microscopy and biomass quantification revealed that under static culture conditions with liquid M63 media containing glycerol, *E. coli* MG1655 *ompR234* ("*ompR234*"), which has an intact endogenous *csgA* gene, formed thick adherent biofilms. However, cells with the *csgA* gene knocked out and no *csgA*-expressing circuits ("Δ*csgA ompR234*"), and aTc$_{Receiver}$/CsgA$_{His}$ cells in the absence of aTc, did not form biofilms. In contrast, inducing aTc$_{Receiver}$/CsgA$_{His}$ cells with aTc resulted in the formation of thick adherent biofilms. **b,** Confocal microscopy and biomass quantification revealed similar biofilm-forming capabilities by MG1655 *ompR234* and induced aTc$_{Receiver}$/CsgA$_{His}$ cells when grown in flow cells with liquid M63 media containing glycerol. In this figure, a) and b) are complementary experiments to those shown in Fig. 1c and 1d, which used liquid M63 media with glucose; here, we used liquid M63 media with glycerol. To enable visualization, we transformed a constitutive mCherry-expressing plasmid into all strains (see Supplementary Methods). Orthogonal XZ and YZ views are maximum-intensity projections. Scale bars are 50μm.

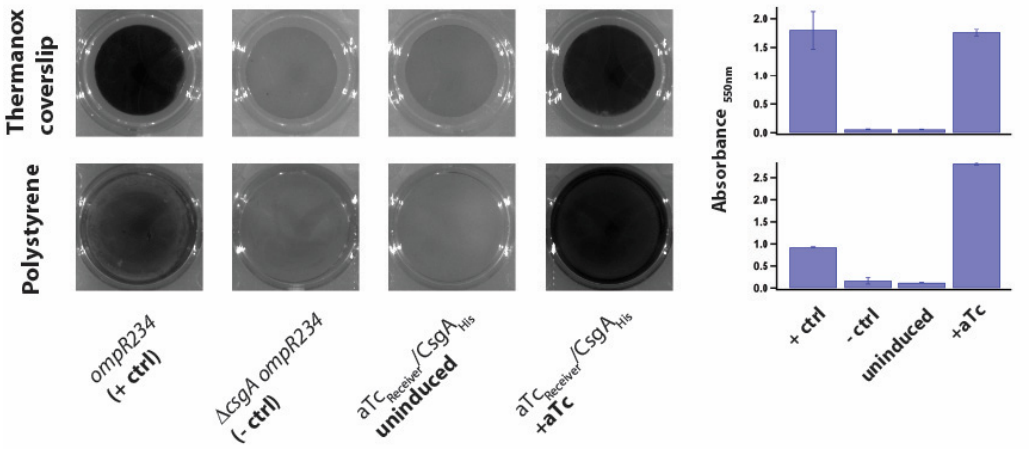

Supplementary Figure 3 | Crystal Violet (CV) staining revealed that under static culture conditions with liquid M63 containing glucose, no biofilms were formed by $aTc_{Receiver}/CsgA_{His}$ cells in the absence of aTc, or by cells with the *csgA* gene knocked out (MG1655 *PRO* Δ*csgA ompR234*). In contrast, adherent biofilms are formed by $aTc_{Receiver}/CsgA_{His}$ cells in the presence of aTc, and by *E. coli* MG1655 *ompR234*. CV staining was quantified by absorbance at 550nm.

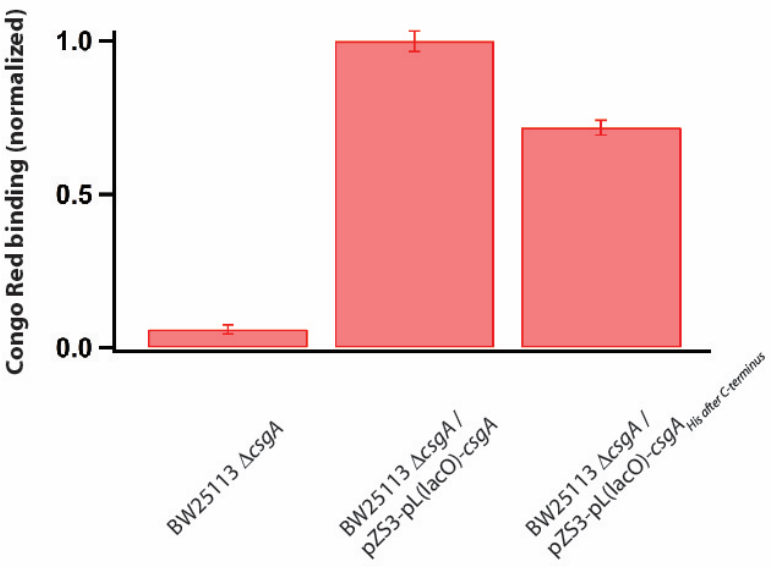

Supplementary Figure 4 | Quantitative Congo Red (CR) binding assay of BW25113 Δ*csgA* cells, cells expressing CsgA (BW25113 Δ*csgA* / pZS3-pL(lacO)-*csgA*), and cells expressing CsgA with a His tag fused to the C-terminus (BW25113 Δ*csgA* / pZS3-pL(lacO)-*csgA*$_{His\ after\ C\text{-}terminus}$) shows that CsgA maintains ability to form amyloid fibrils after fusion of peptides to the C-terminus.

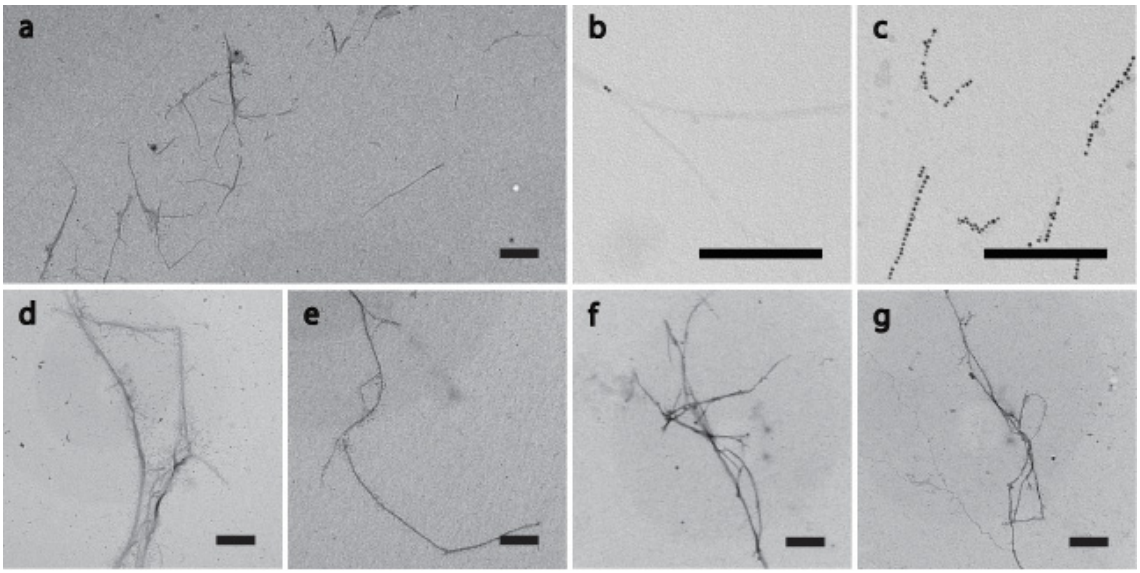

Supplementary Figure 5 | Fibrils imaged with TEM are CsgA-based fibrils and histidine tag addition to CsgA does not interfere with fibril production. Histidine tags confer specific NiNTA gold particle (NiNTA-AuNP) binding functionality. Fibrils produced by engineered cell strains grown with chemical induction (**b-g**) have similar morphology to CsgA-based curli fibrils described in Chapman *et al.*[1] as well as **a,** curli fibrils produced by *E. coli* MG1655 *ompR234*. **b,** There was no specific labelling of CsgA fibrils with NiNTA-AuNPs in the absence of histidine tags on CsgA (fibrils produced by induced $aTc_{Receiver}$/CsgA cells). **c,** Curli fibrils were specifically labelled by NiNTA-AuNPs when histidine tags were added to CsgA (fibrils produced by induced $aTc_{Receiver}$/$CsgA_{His}$ cells). Furthermore, histidine tag addition to CsgA did not interfere with curli fibril production. **d,** Engineered cells expressing CsgA when induced by AHL ($AHL_{Receiver}$/CsgA) produced fibrils, as did **e,** engineered cells expressing $CsgA_{His}$ when induced by AHL ($AHL_{Receiver}$/$CsgA_{His}$). **f,** Engineered cells expressing CsgA when induced by aTc ($aTc_{Receiver}$/CsgA) produced fibrils, as did **g,** engineered cells expressing $CsgA_{His}$ when induced by aTc ($aTc_{Receiver}$/$CsgA_{His}$). Scale bars are 200nm.

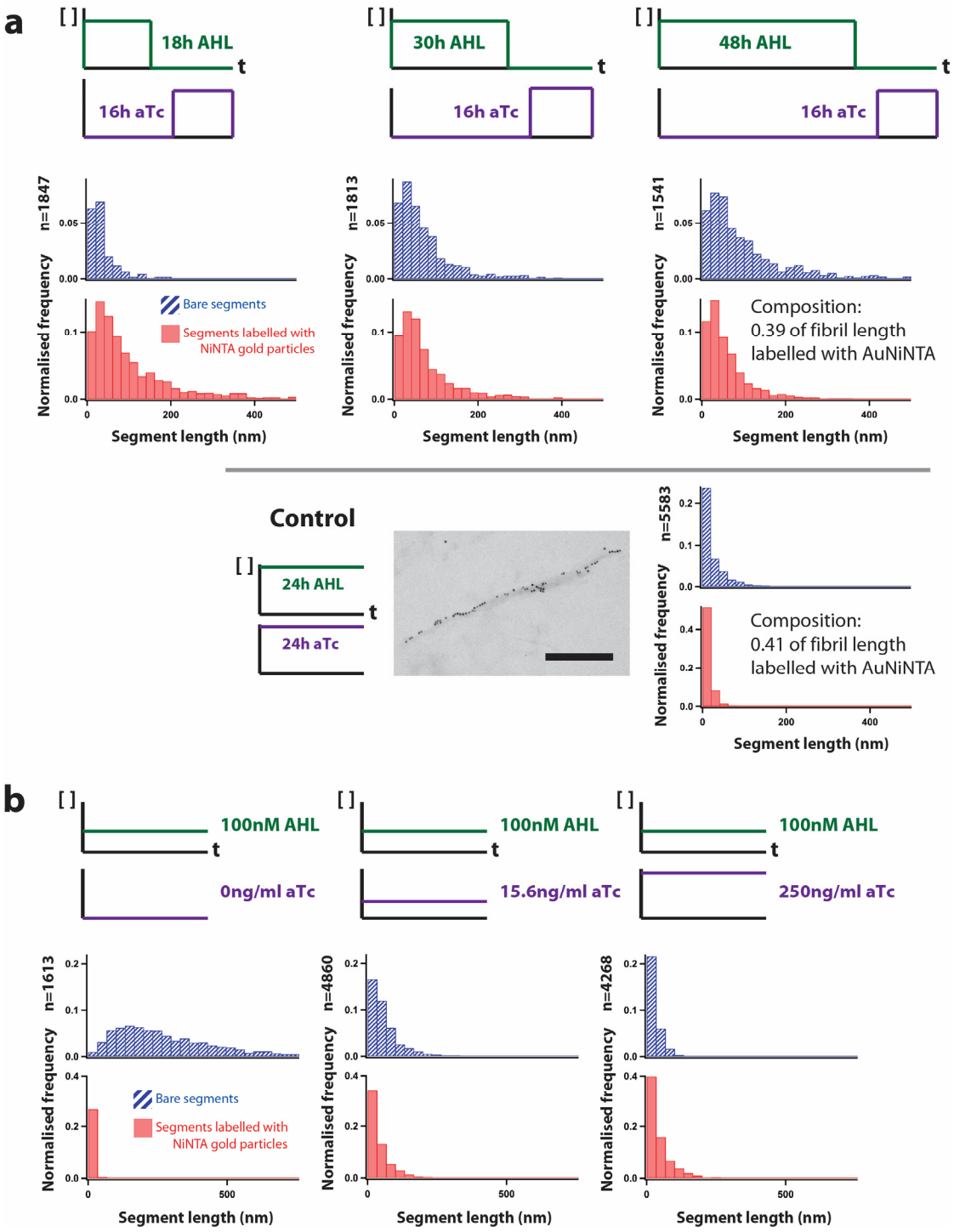

Supplementary Figure 6 | Tuning the length distribution of CsgA and $CsgA_{His}$ blocks by changing temporal interval lengths and amplitudes of input signals. **a,** Histogram data corresponding to TEM images in Fig. 2b. The segments in block co-fibrils were longer than those in co-fibrils assembled when CsgA and $CsgA_{His}$ were secreted simultaneously with no

temporal separation (Control), even though both types of materials had similar ratios of CsgA to $CsgA_{His}$. Scale bar is 200nm. **b,** Histogram data corresponding to TEM images in Fig. 2d. Hashed blue bars indicate bare segments of amyloid fibrils that were unlabelled by NiNTA-AuNPs, while solid red bars indicate amyloid fibril segments labelled with NiNTA-AuNPs.

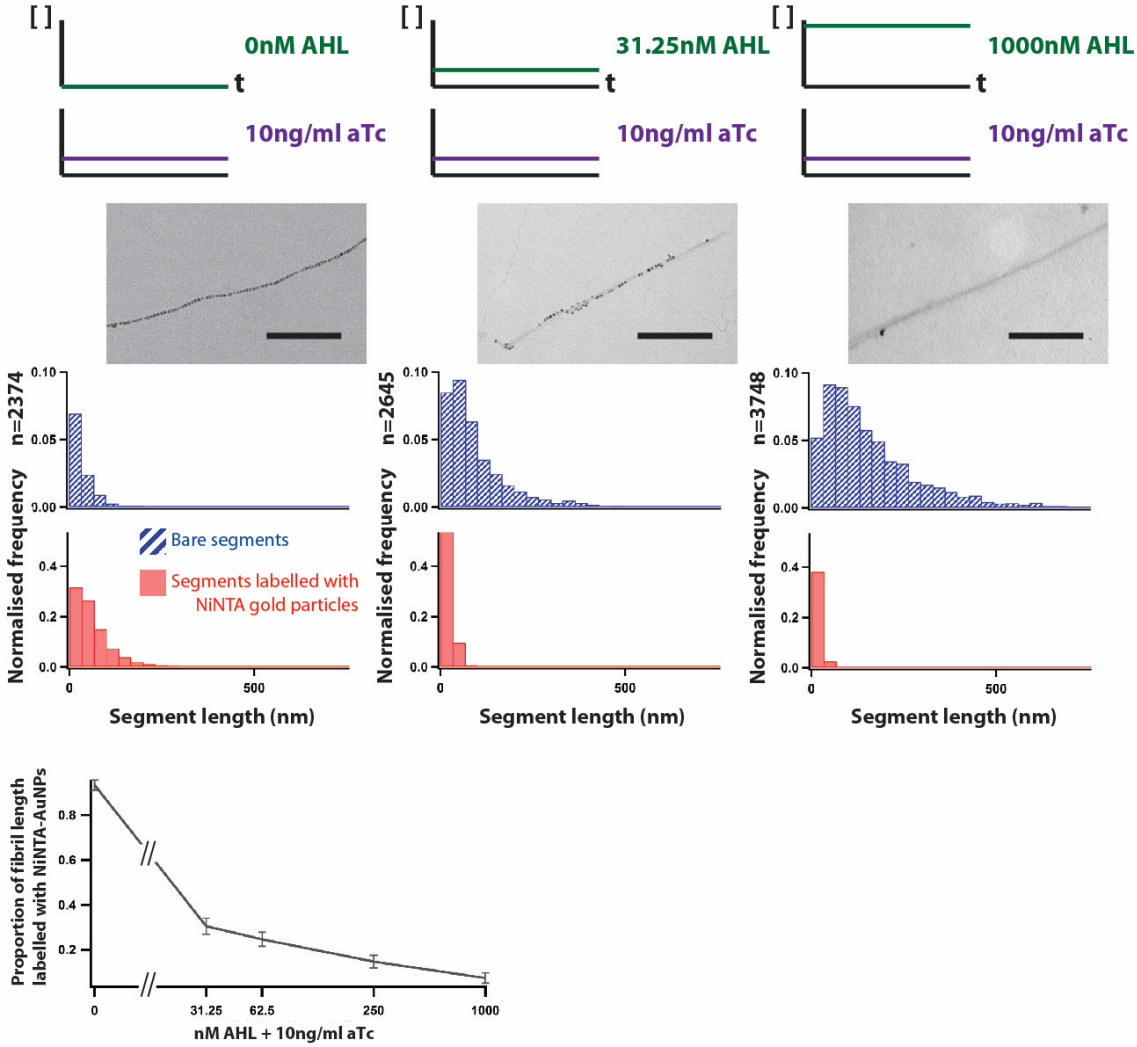

Supplementary Figure 7 | Conversion of chemical inducer amplitude to material structure and composition. Complementary experiment to that described in Fig. 2d. With synthetic gene circuits, cells can translate the amplitude of input signals into nanoscale structure and composition of block co-fibrils. AHL induces secretion of CsgA from $AHL_{Receiver}$/CsgA, while at the same time, aTc induces secretion of $CsgA_{His}$ from $aTc_{Receiver}$/$CsgA_{His}$. We tuned the length distributions of the CsgA and $CsgA_{His}$ blocks, as well as the relative proportions of CsgA and $CsgA_{His}$, by changing the relative concentration of simultaneously applied AHL and aTc inducers. Hashed blue bars indicate bare segments of amyloid fibrils that were unlabelled, while solid red bars indicate amyloid fibril segments labelled with NiNTA-AuNPs. Solid grey line indicates the proportion of fibril length labelled by NiNTA-AuNPs. Scale bars are 200nm.

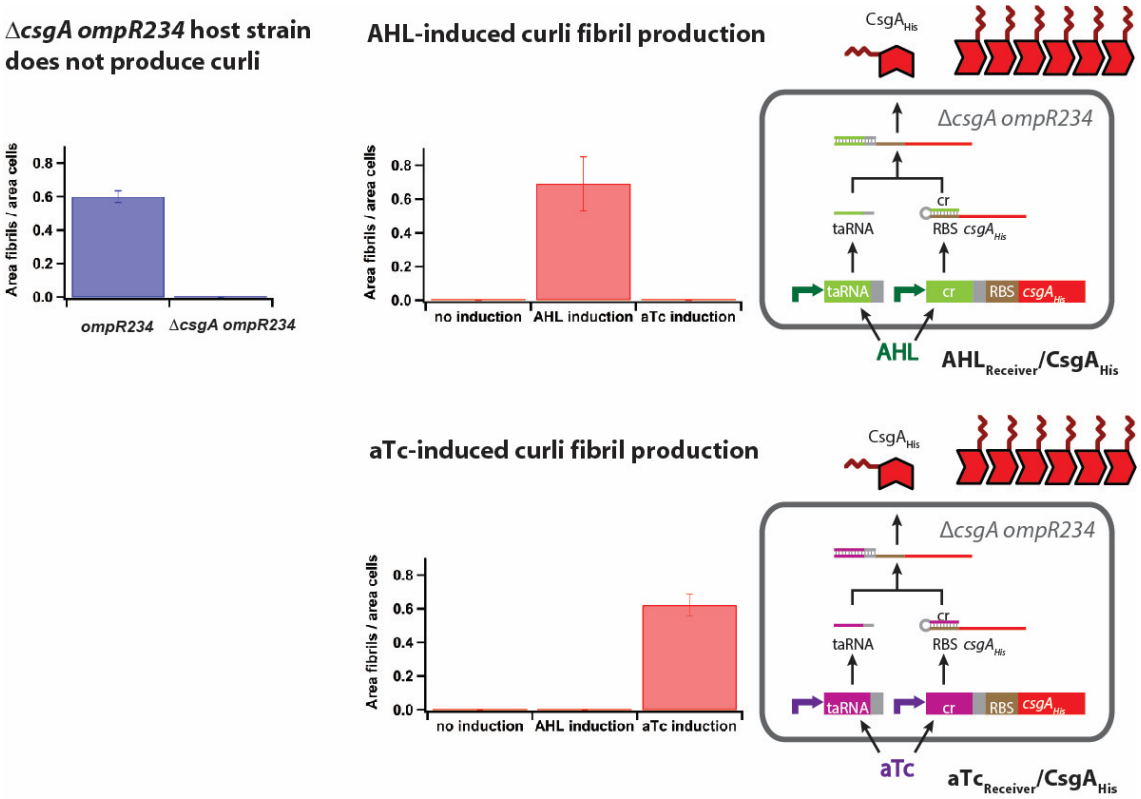

Supplementary Figure 8 | Engineered *E. coli* only produce curli fibrils when induced by the correct inducer. The curli knockout host strain used to create engineered inducer-responsive strains, *E. coli* MG1655 *PRO ΔcsgA ompR234* ("Δ*csgA ompR234*"), does not produce curli fibrils. In contrast, the *E. coli* MG1655 *ompR234* ("*ompR234*") strain does. The AHL-responsive engineered strain ($AHL_{Receiver}$/$CsgA_{His}$) only produces curli fibrils when induced by AHL. The aTc-responsive engineered strain ($aTc_{Receiver}$/$CsgA_{His}$) only produces curli fibrils when induced by aTc. Curli fibril production was quantified by taking the ratio of area of fibrils to area of cells in TEM images analysed by ImageJ.

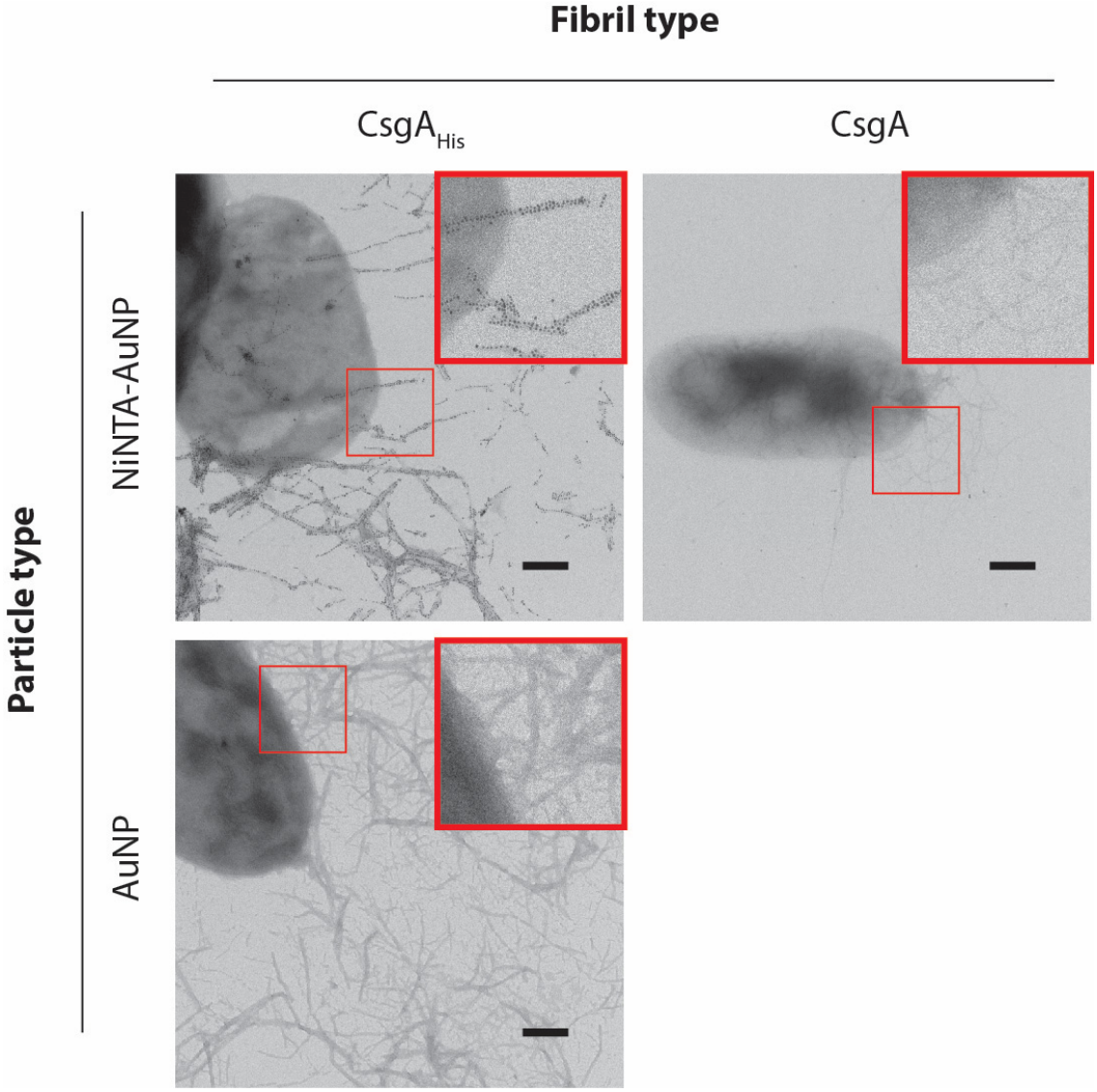

Supplementary Figure 9 | The interaction between NiNTA-AuNPs and His-tagged curli fibrils is specific. His-tagged CsgA fibrils (CsgA$_{His}$) bound NiNTA-AuNPs but wild-type CsgA fibrils did not, indicating that the His tag was necessary for this interaction. Moreover, gold particles without NiNTA conjugation (AuNP) did not bind His-tagged CsgA fibrils, indicating that NiNTA groups were also required for this interaction. The images outlined by thick red boxes are zoomed-in versions of regions outlined by the smaller red boxes. Scale bars are 200nm.

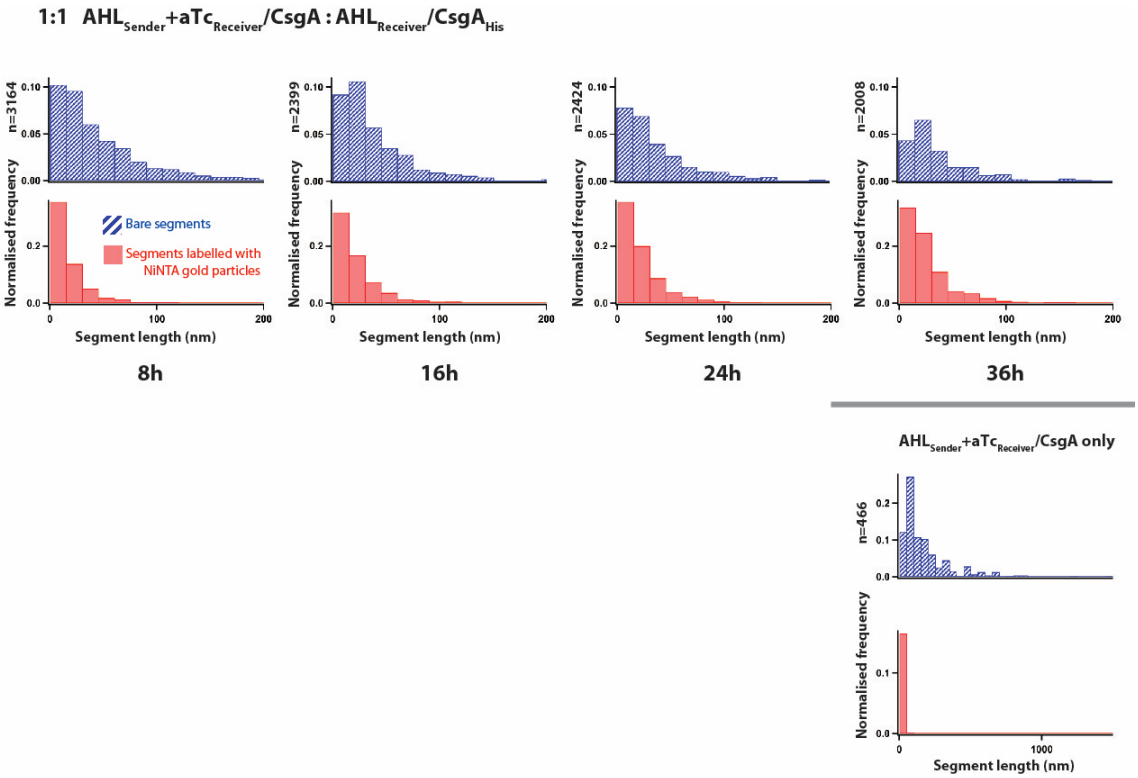

Supplementary Figure 10 | Histogram data corresponding to the TEM images in Fig. 3b. This data shows that the length distribution of CsgA and $CsgA_{His}$ blocks changed with time when curli synthesis was regulated by autonomous cellular communication circuits. Hashed blue bars indicate bare segments of amyloid fibrils that were unlabelled by NiNTA-AuNPs, while solid red bars indicate amyloid fibril segments labelled with NiNTA-AuNPs.

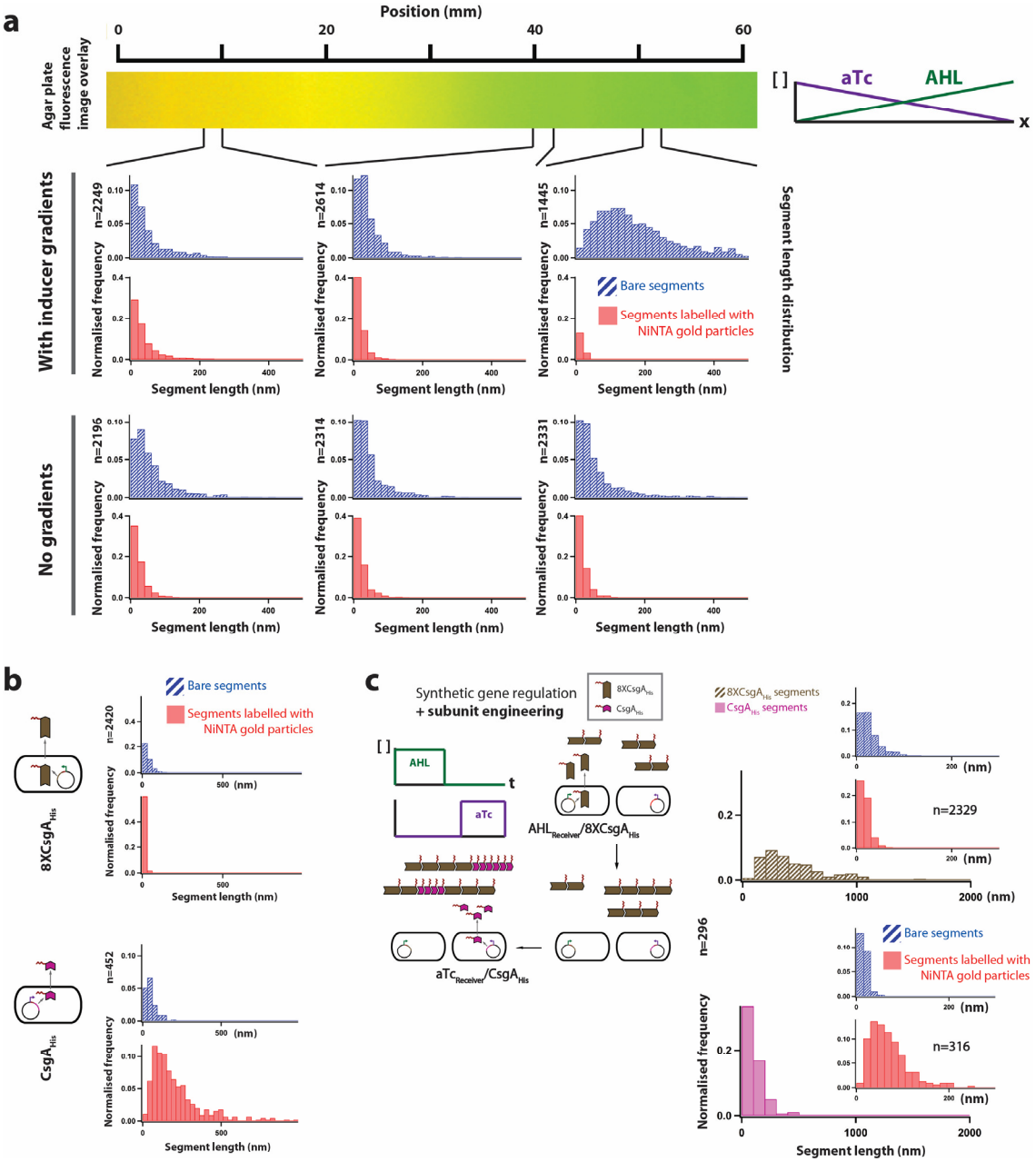

Supplementary Figure 11 | a, Histogram data corresponding to TEM images in Fig. 4b. This data shows that the length distribution of CsgA and CsgA$_{His}$ blocks changed across the agar plate when inducer concentration gradients were present, but not in the absence of gradients. Hashed blue bars indicate bare segments of amyloid fibrils that were unlabelled by NiNTA-AuNPs, while solid red bars indicate amyloid fibril segments labelled with NiNTA-AuNPs. **b,** Histogram data corresponding to TEM images in Fig. 4c. This data shows that CsgA$_{His}$ and 8XCsgA$_{His}$ fibrils organized NiNTA-AuNPs in different distributions. Hashed blue bars

indicate bare segments of amyloid fibrils that were unlabelled by NiNTA-AuNPs, while solid red bars indicate amyloid fibril segments labelled with NiNTA-AuNPs. **c,** Histogram data corresponding to TEM images in Fig. 4d. The length distributions of 8XCsgA$_{His}$ segments and CsgA$_{His}$ segments are shown in histograms with hashed brown bars and solid amethyst bars, respectively. Inset histograms show the length distributions of unlabelled segments (hashed blue bars) and segments labelled with NiNTA-AuNPs (solid red bars) for both the 8XCsgA$_{His}$ segments and the CsgA$_{His}$ segments.

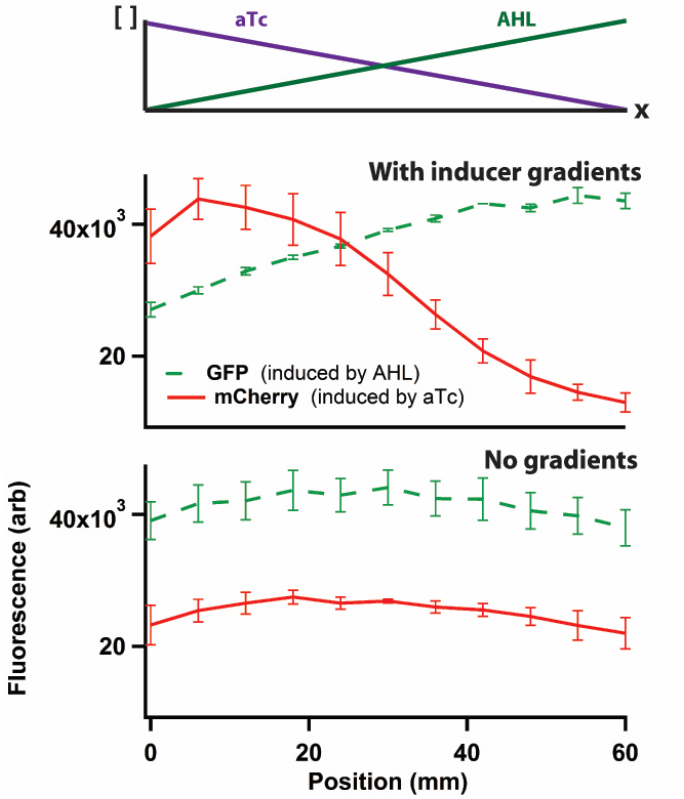

Supplementary Figure 12 | Inducer gradient visualization for agar plates described in Fig. 4a and Fig. 4b. Top-agar-embedded $AHL_{Receiver}$/GFP reporter cells (dashed green lines) and $aTc_{Receiver}$/mCherry reporter cells (solid red lines) enabled the visualization of inducer concentration gradients across the agar plate.

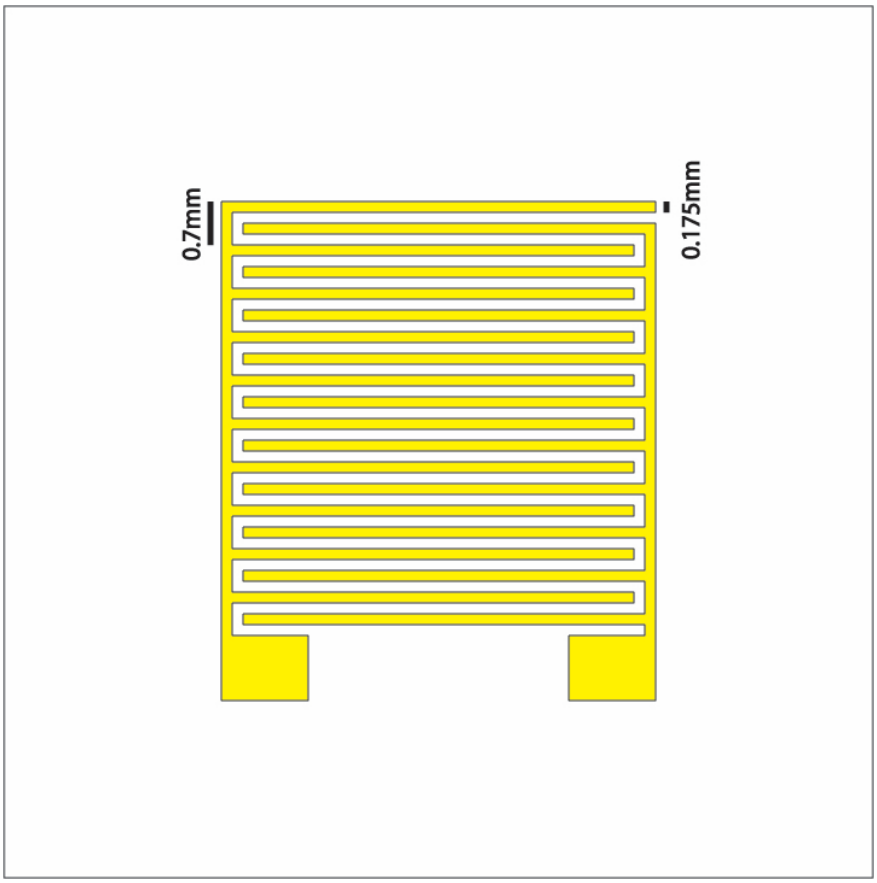

Supplementary Figure 13 | Shadowing mask used to make interdigitated electrodes. The two continuous yellow regions represent holes in the mask through which gold was shadowed to create the electrodes.

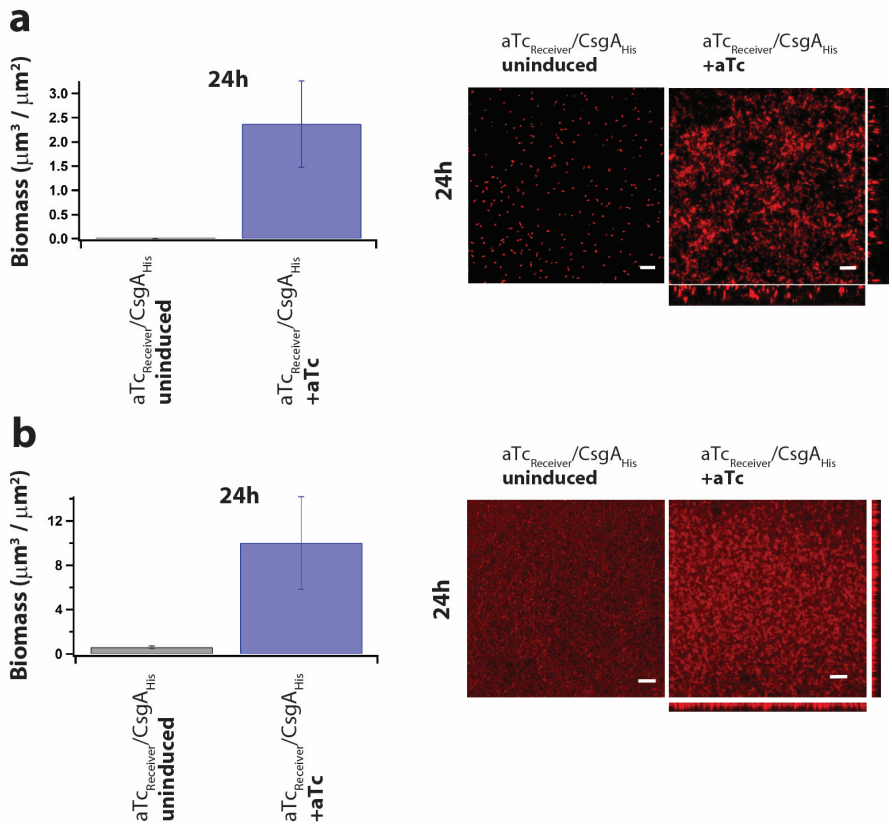

Supplementary Figure 14 | a, Confocal microscopy and biomass quantification revealed thick biofilms formed by aTc-induced $aTc_{Receiver}/CsgA_{His}$ cells by 24 hours when grown with 100nM NiNTA-AuNP in liquid M63 media containing glucose, under static culture conditions. To enable visualization, we transformed a constitutive mCherry-expressing plasmid into this strain (see Supplementary Methods). **b,** The same was observed under flow conditions. Scale bars are 50μm.

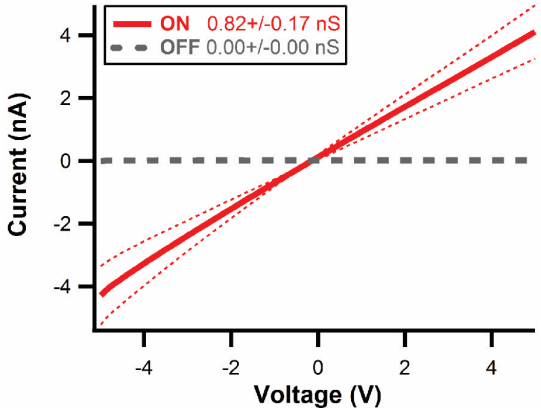

Supplementary Figure 15 | The aTc-induced 'ON' state for $aTc_{Receiver}$/$CsgA_{His}$ biofilms exhibited a conductance of 0.82±0.17 (s.e.m.) nS (solid red line), while the 'OFF' state had no measureable conductance (dashed grey line).

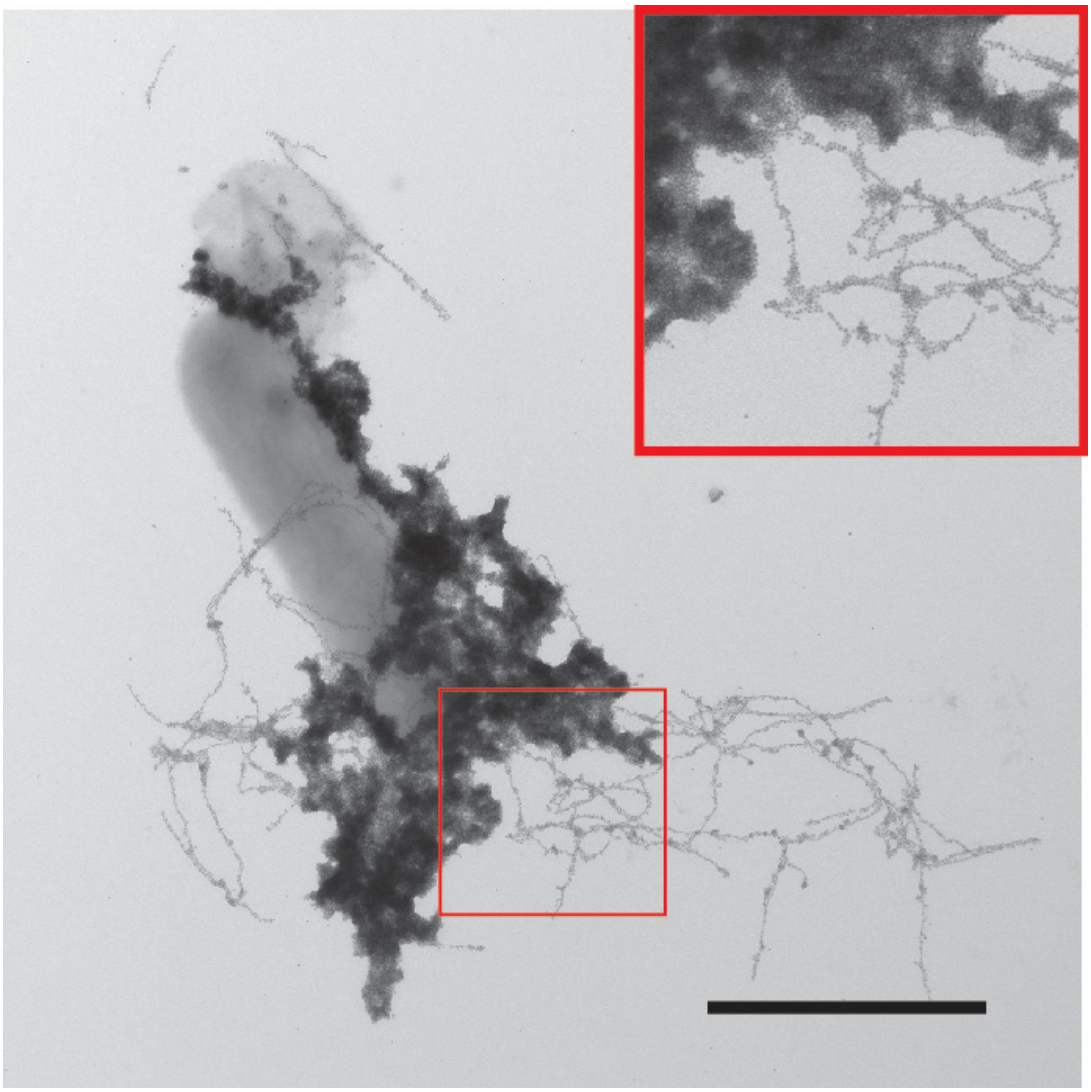

Supplementary Figure 16 | TEM shows that aTc-induced $aTc_{Receiver}$/$CsgA_{His}$ cells produced curli fibrils that organized NiNTA-AuNPs into dense networks (the 'ON' state). This is complementary data to TEM images show in Fig. 5b. The image outlined by the thick red box is a zoomed-in version of the region outlined by the small red box. Scale bar is 1μm.

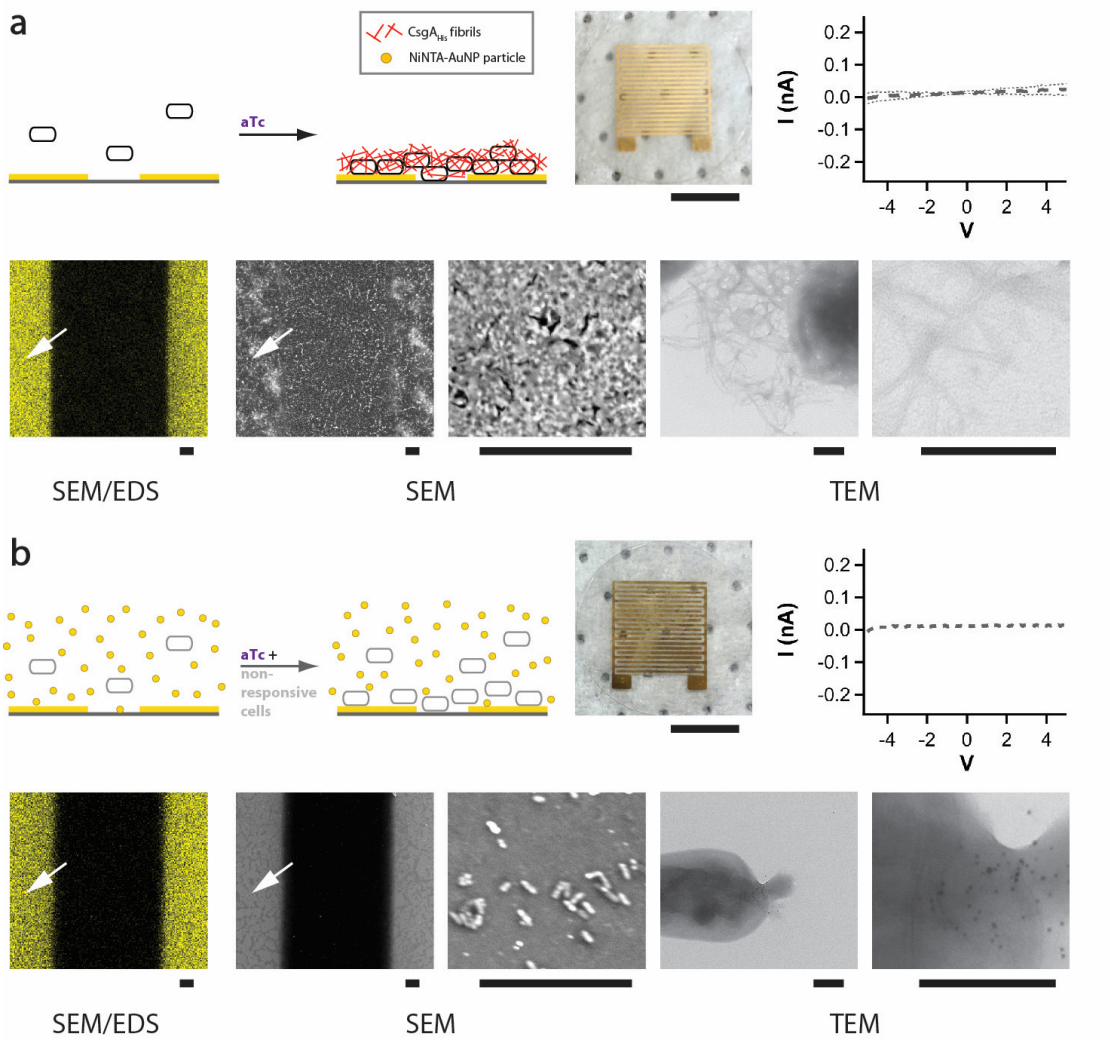

Supplementary Figure 17 | Additional negative controls for chemical-inducer-switchable conductive biofilms show in Figure 5. **a,** When aTc$_{Receiver}$/CsgA$_{His}$ biofilms were grown with aTc induction but without NiNTA-AuNPs, conductance was 2.4±3.5 (s.e.m.) pS. SEM/EDS showed no gold networks connecting electrodes (white arrows) even though SEM imaging showed that thick biofilms spanned electrodes. TEM imaging showed that curli fibrils were present, but without gold particles. **b,** Populations of cells which do not respond to aTc (AHL$_{Receiver}$/CsgA$_{His}$) were not conductive in the presence of aTc and NiNTA-AuNPs. SEM/EDS showed no gold networks connecting electrodes and SEM imaging showed only scattered cells in the gap between electrodes. TEM imaging showed no curli fibrils and only scattered, isolated gold particles. Scale bars of digital photographs are 5mm, scale bars of

scanning electron micrographs are 20μm, and scale bars of transmission electron micrographs are 200nm.

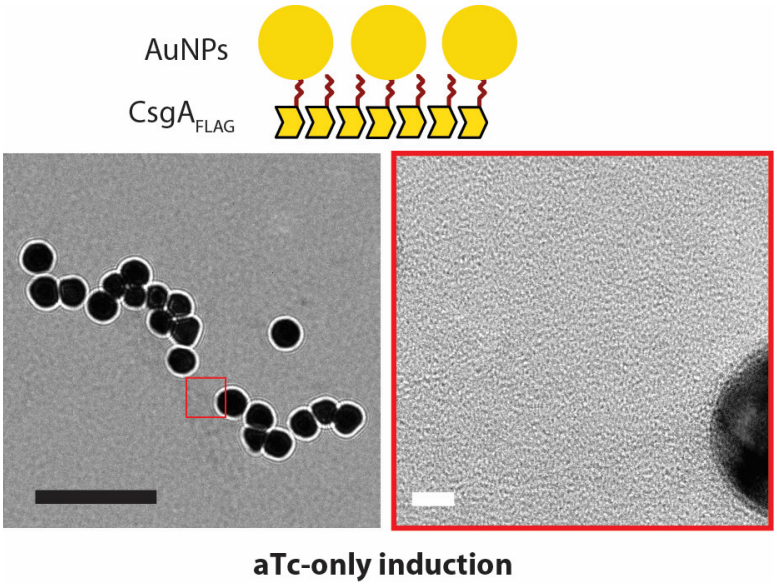

Supplementary Figure 18 | A mixed population of aTc$_{Receiver}$/CsgA$_{FLAG}$ and AHL$_{Receiver}$/CsgA$_{SpyTag}$ cells produced curli templates for AuNP-only assemblies (CsgA$_{FLAG}$ fibrils) when induced by aTc only. FLAG tags displayed on fibrils specifically bound anti-FLAG antibodies which were in turn bound by AuNPs conjugated to secondary antibodies. The image on the right is the zoomed-in version of the inset red box on the left. Black scale bars are 200nm and white scale bars are 5nm.

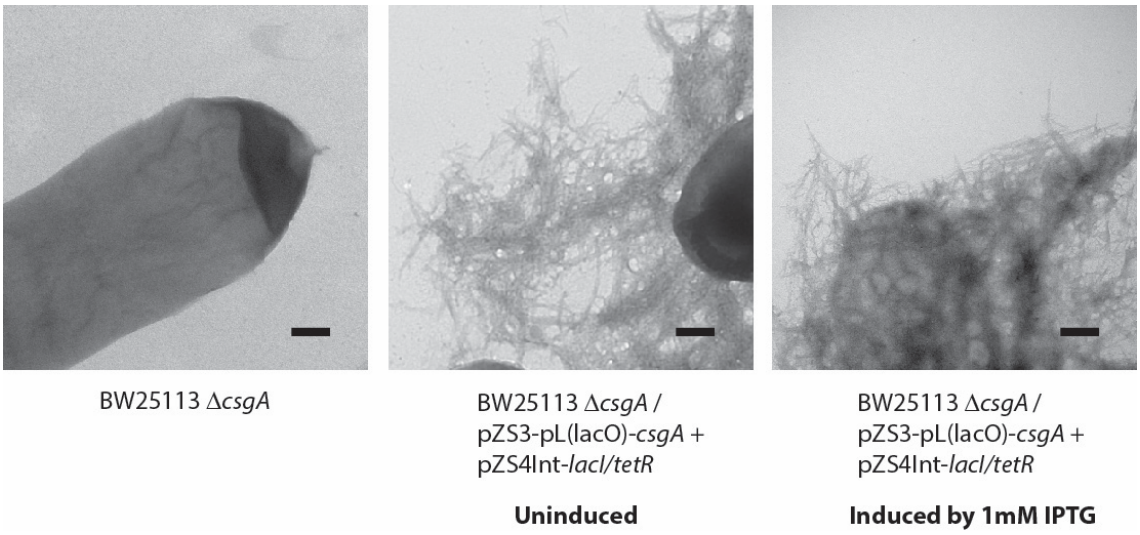

Supplementary Figure 19 | Synthetic riboregulators enable tight regulation of curli subunit expression, which is important for patterning (Figs. 2-4). When the only means of control of *csgA* gene expression was a pL(lacO) promoter controlling the downstream *csgA* gene (with no riboregulators) in cells expressing the LacI repressor (BW25113 Δ*csgA* / pZS3-pL(lacO)-*csgA* + pZS4Int-*lacI/tetR*), curli fibrils were seen in the absence as well as in the presence of IPTG inducer, making such a system not suitable for patterning. Scale bars are 200nm.

a

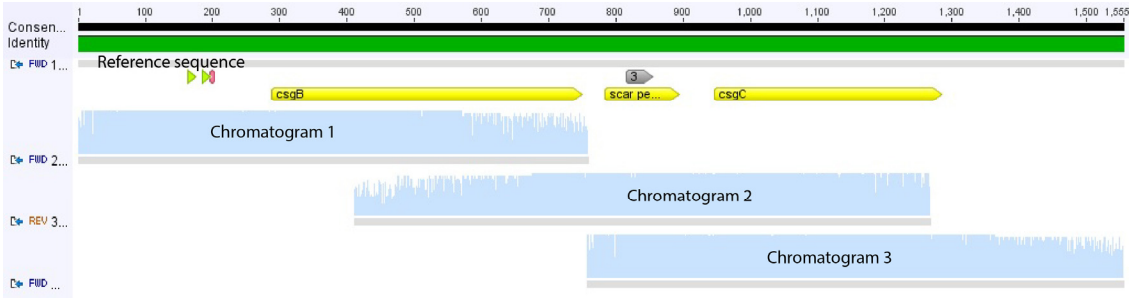
Consen...
Identity
FWD 1...
Reference sequence
csgB
scar pe...
csgC
Chromatogram 1
FWD 2...
Chromatogram 2
REV 3...
Chromatogram 3
FWD ...

b

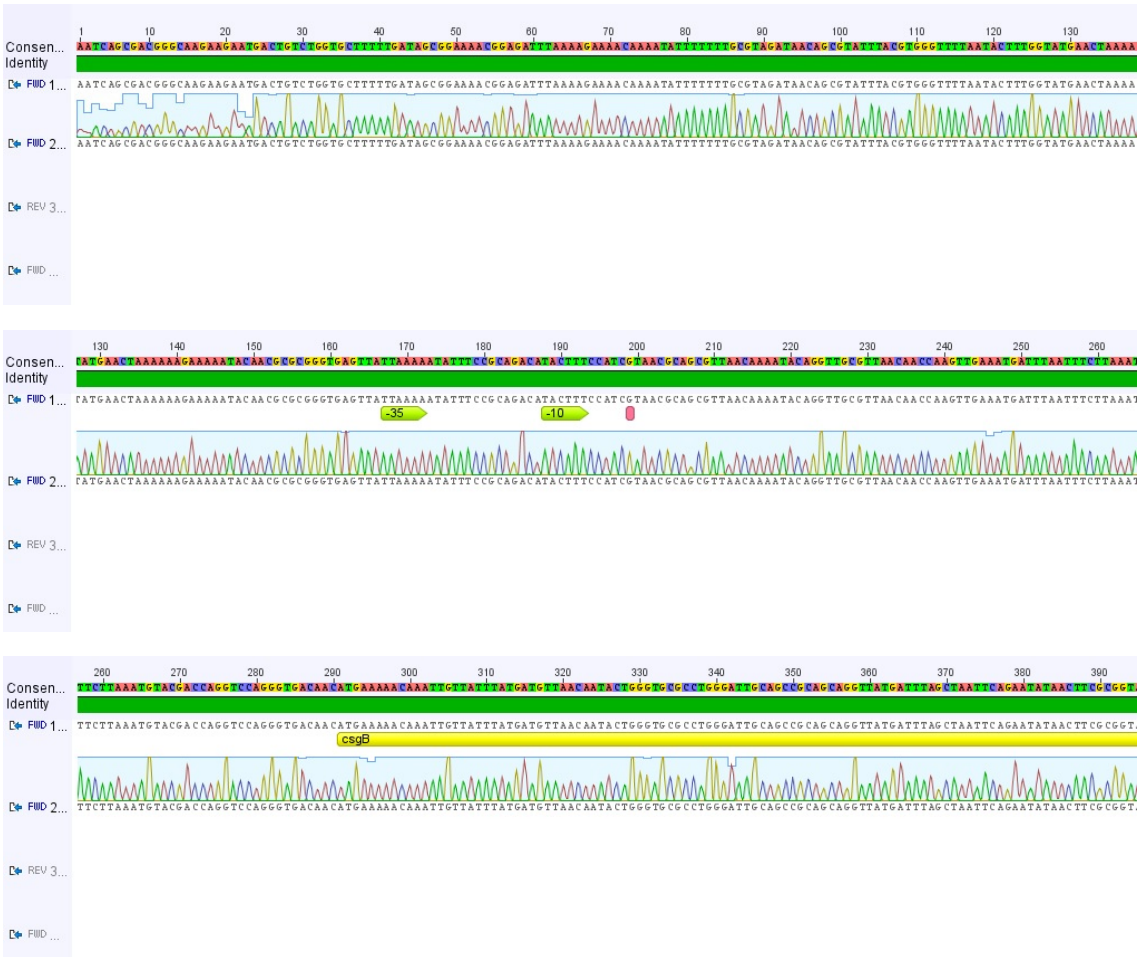
Consen...
Identity
FWD 1...
FWD 2...
REV 3...
FWD ...
-35
-10
csgB

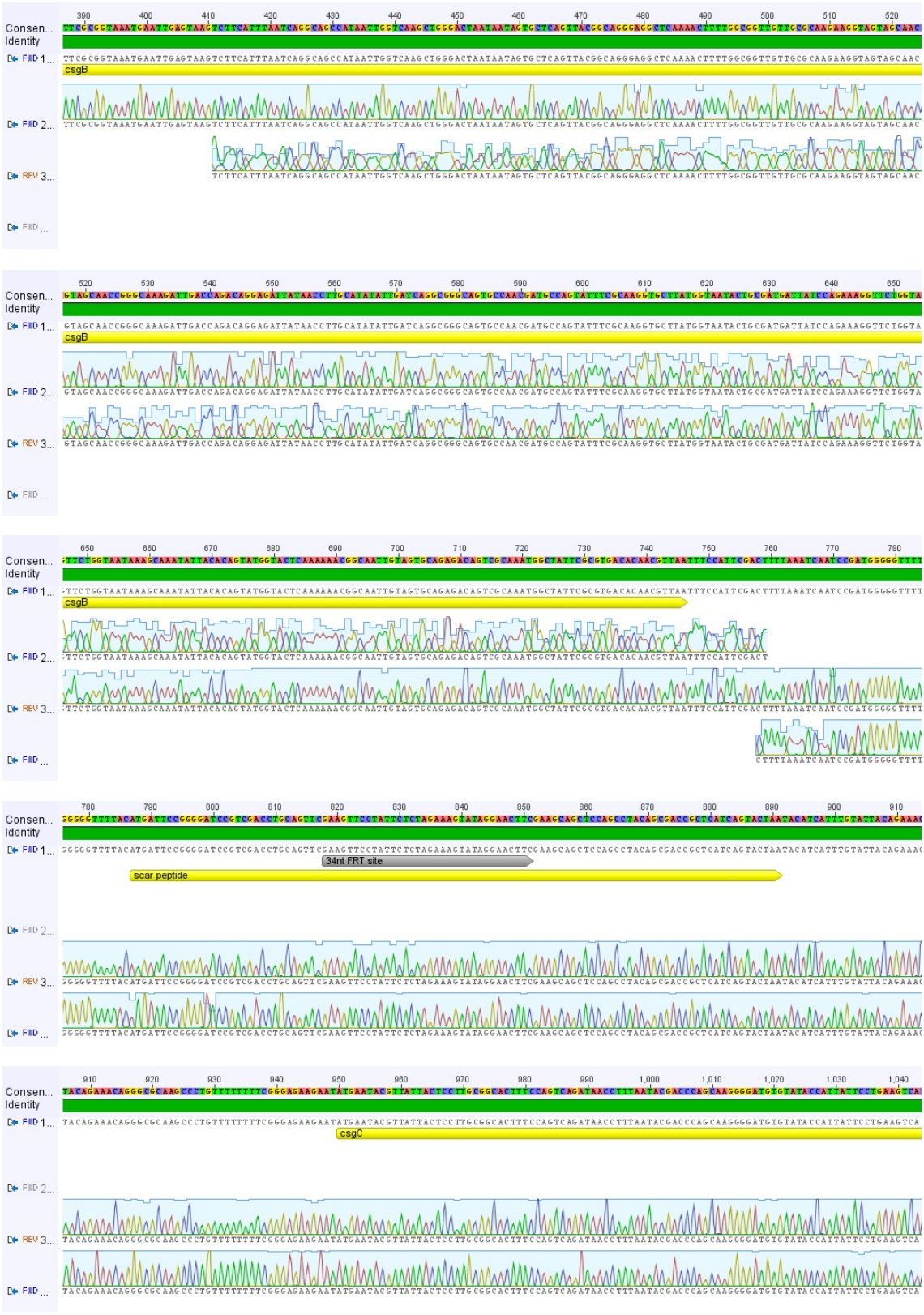
Consen...
Identity
FWD 1...
csgB
FWD 2...
REV 3...
FWD ...
34nt FRT site
scar peptide
csgC

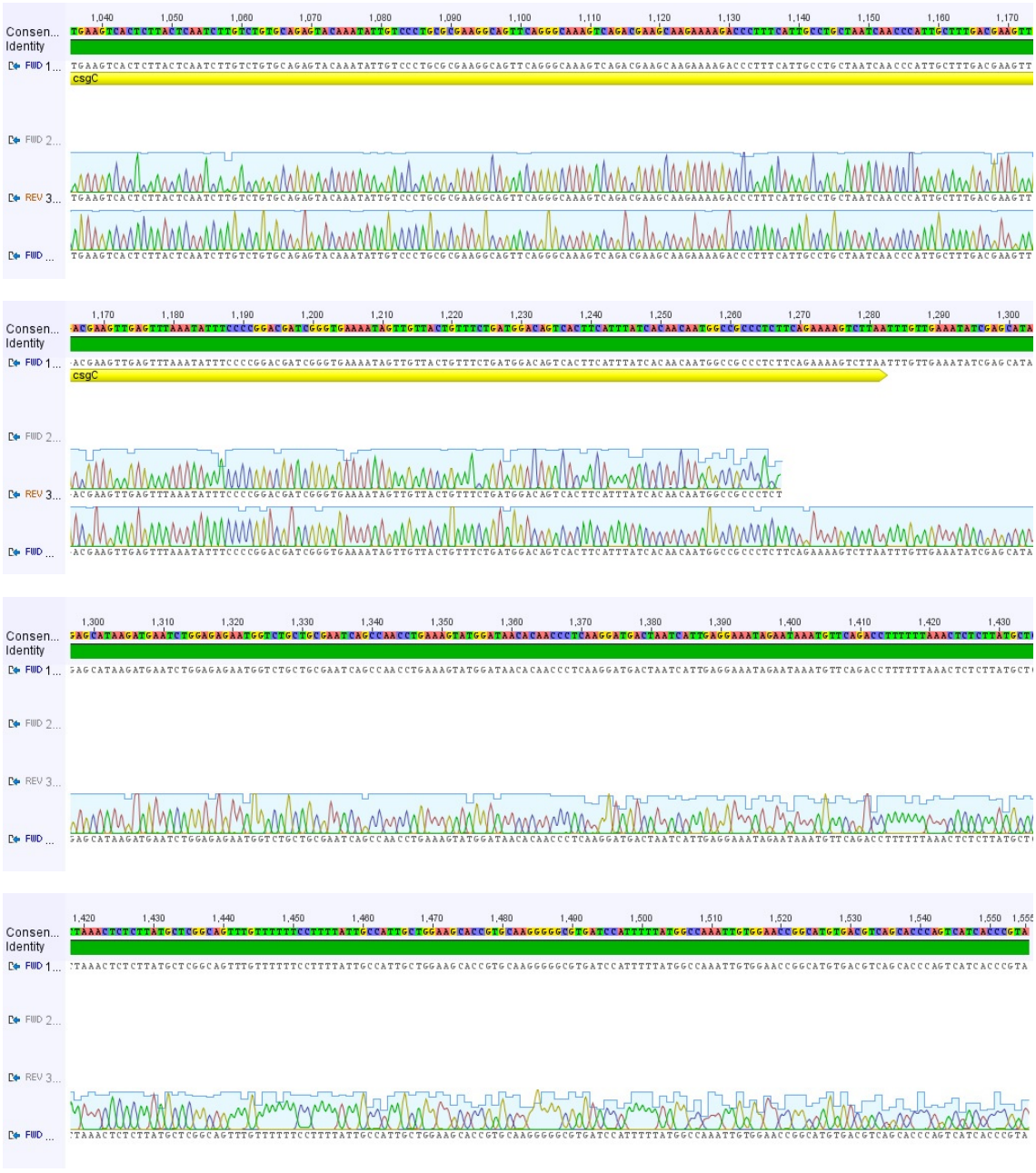

Supplementary Figure 20 | Sequencing results of the PCR product from the *csgBAC* operon of *E. coli* MG1655 *PRO* Δ*csgA ompR234* show that *csgA* was deleted and replaced by a scar sequence, while *csgB* and *csgC* are intact. Moreover, the promoter for *csgB* is present. **a,** The zoomed-out sequencing results showing an overview of the sequenced operon. **b,** The zoomed-in sequencing results showing the underlying DNA sequences. The consensus sequence obtained from integrating three sequencing reactions is the sequence above the green bar. The sequence just below the green bar represents the reference sequence, which is

further annotated with yellow, grey, and green arrows representing genes, FRT sites, and promoter elements, respectively. The green bar below the consensus sequence indicates that the sequencing results match the reference sequence.

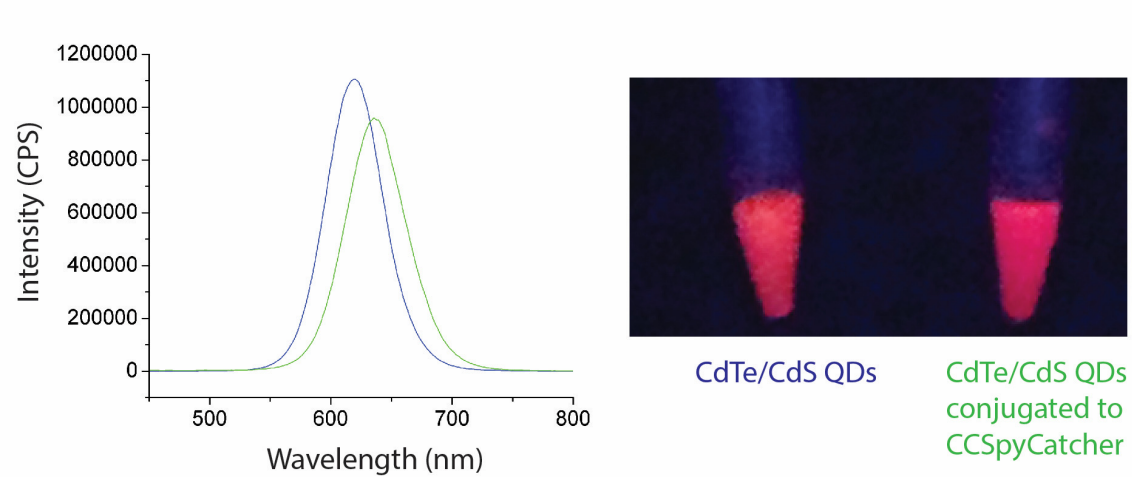

Supplementary Figure 21 | Photoluminescence spectra and real-color pictures of CdTe/CdS quantum dots before (left blue curve, emission peak at 620nm) and after (right green curve, emission peak at 638nm) conjugation with CCSpyCatcher protein show that CdTe/CdS QDs remained highly fluorescent after conjugation. Photoluminescence spectra were obtained under excitation at 450nm (NanoLog Spectrometer, HORIBA Jobin Yvon). Real-color pictures were obtained under excitation at 365nm (UV lamp).

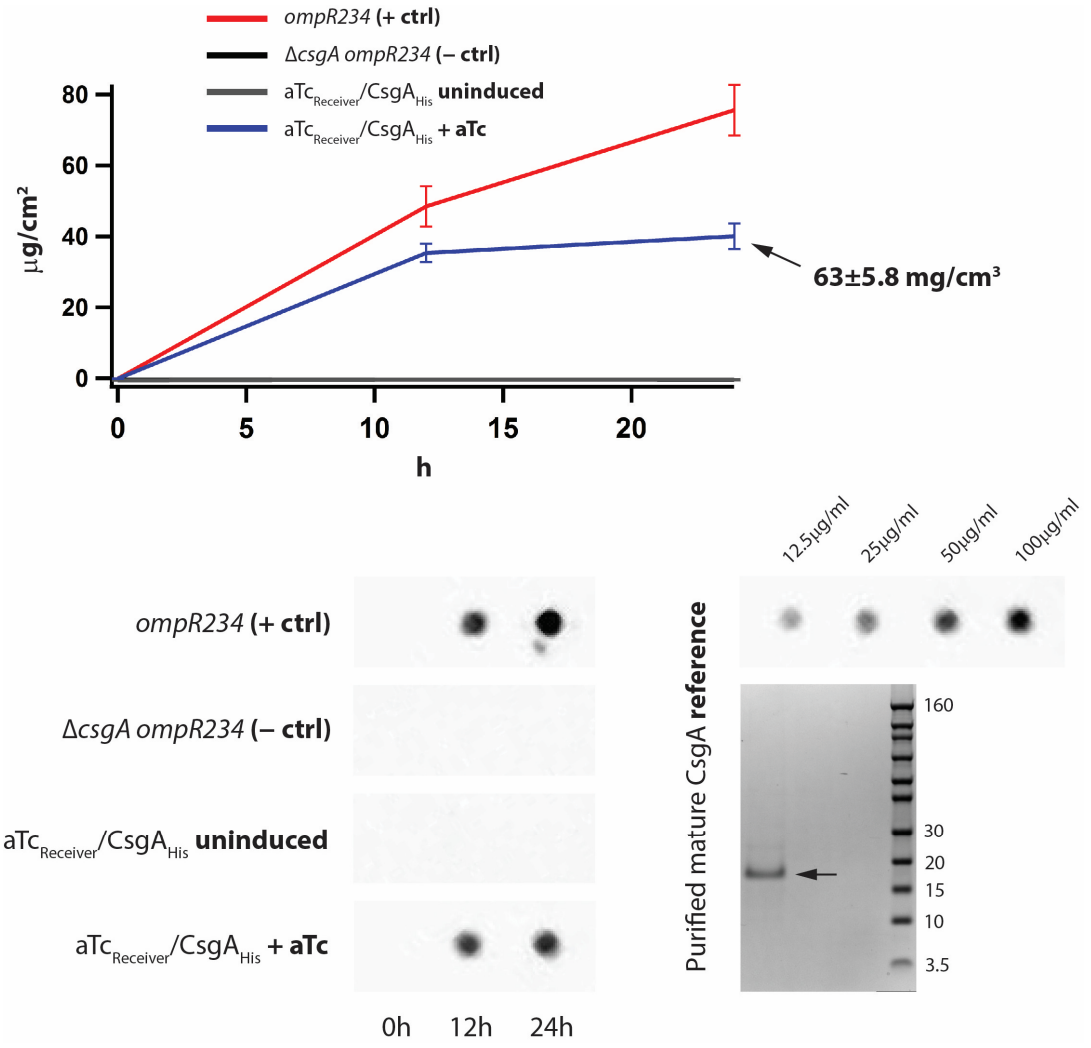

Supplementary Figure 22 | Dot blot quantitation of CsgA production in biofilms. We quantitated CsgA with anti-CsgA antibody and found no signal from cultures of MG1655 *PRO ΔcsgA ompR234* cells ("– ctrl") or uninduced $aTc_{Receiver}/CsgA_{His}$ cells. In contrast, $aTc_{Receiver}/CsgA_{His}$ cells induced with 250ng/ml aTc gave no signal at 0h, but at later timepoints gave signal corresponding to 30-40μg of CsgA per cm^2 of biofilm (solid blue line). Similarly, positive control MG1655 *ompR234* cells ("+ ctrl") gave no signal at 0h, but at later timepoints gave signal corresponding to 40-80μg of CsgA per cm^2 of biofilm. At the 24h timepoint, we were also able to use biofilm volume as determined by confocal microscopy (Fig. 1c) to calculate 63±5.8 (s.e.m.) mg of CsgA per cm^3 of biofilm generated by the aTc-induced $aTc_{Receiver}/CsgA_{His}$ cells. For calculation of protein concentration in samples, a reference curve was constructed using serial dilutions of purified mature CsgA without the

Sec signal sequence that is cleaved off during secretion. Mature CsgA was checked for purity by running on a SDS-PAGE gel with Coomassie staining. The purified CsgA monomer migrates at a higher apparent MW on the gel, at ~17.5kDa, even though the actual MW is 14.2kDa; this is consistent with results reported in the literature[1].

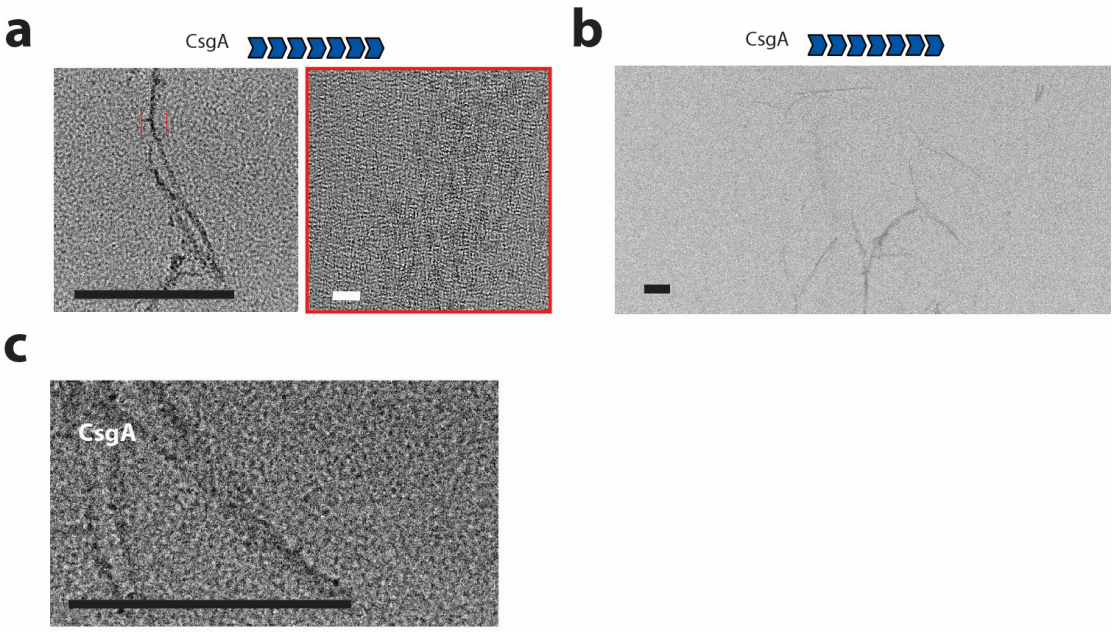

Supplementary Figure 23 | a, CsgA fibrils do not bind CdTe/CdS QDs conjugated to SpyCatcher (negative control for Fig. 6a). **b,** CsgA fibrils do not bind 40nm AuNPs conjugated to antibodies (negative control for Fig. 6a). **c,** CsgA fibrils nucleate few ZnS particles (negative control for Fig. 6d). Black scale bars are 200nm and white scale bars are 5nm; the images outlined by red boxes are zoomed-in versions of the inset red boxes.

Supplementary Figure 24 | Plasmid maps

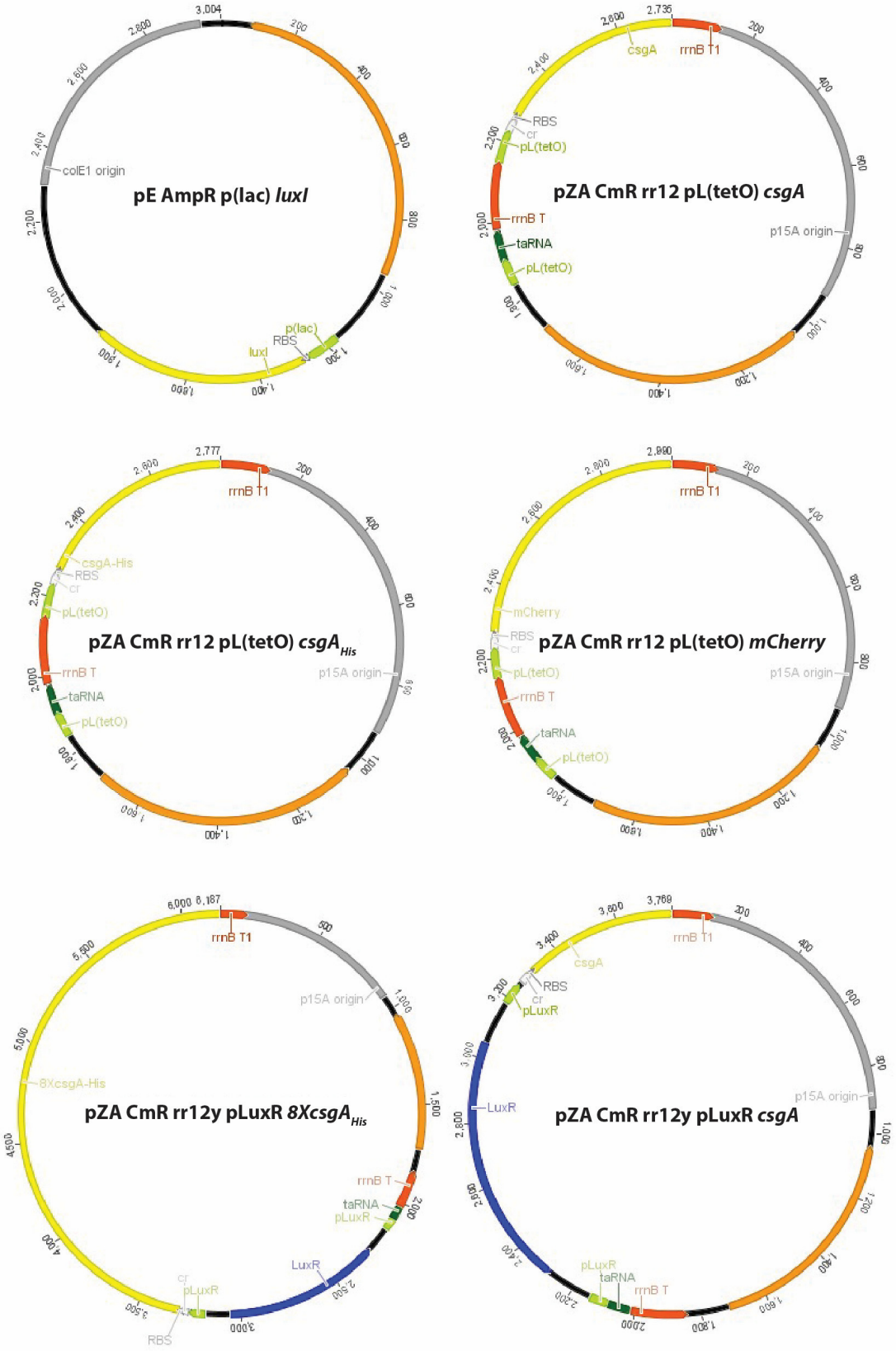

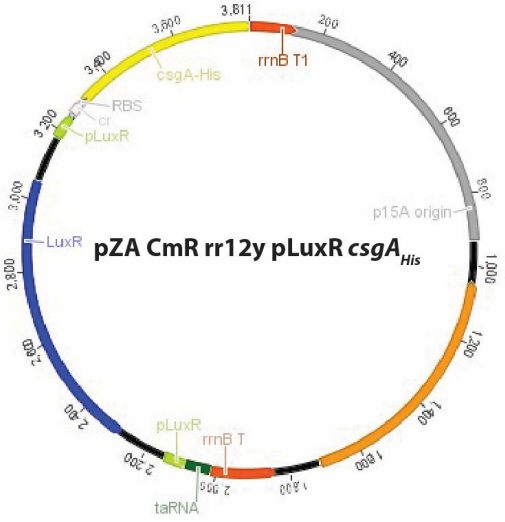
pZA CmR rr12y pLuxR csgA$_{His}$
rrnB T1
csgA-His
RBS
cr
pLuxR
p15A origin
LuxR
pLuxR
rrnB T
taRNA

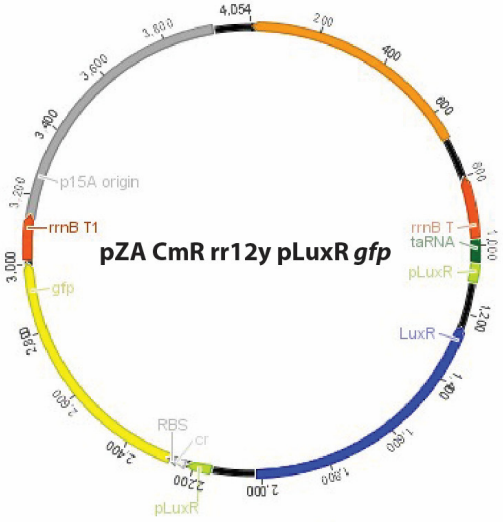
pZA CmR rr12y pLuxR gfp
p15A origin
rrnB T1
rrnB T
taRNA
pLuxR
gfp
LuxR
RBS
cr
pLuxR

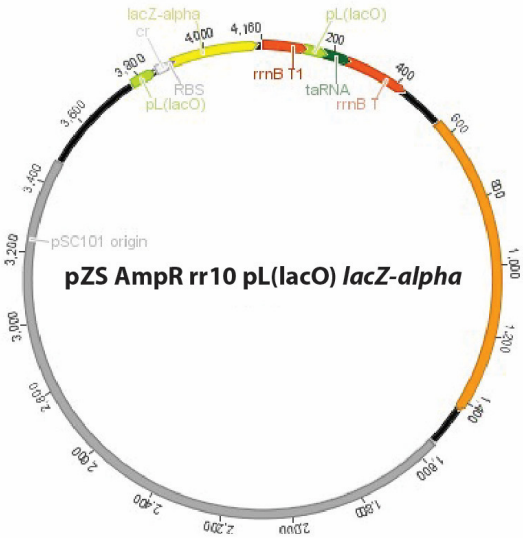
pZS AmpR rr10 pL(lacO) lacZ-alpha
lacZ-alpha
cr
RBS
pL(lacO)
rrnB T1
taRNA
rrnB T
pSC101 origin

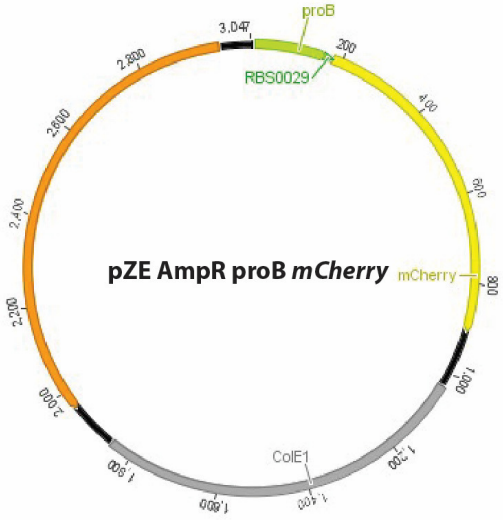
pZE AmpR proB mCherry
proB
RBS0029
mCherry
ColE1

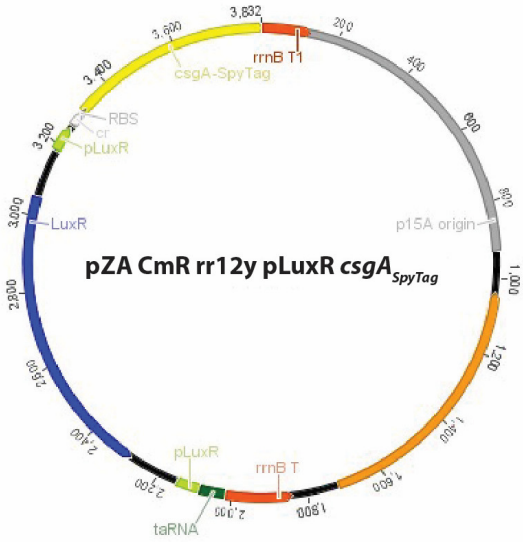
pZA CmR rr12y pLuxR csgA$_{SpyTag}$
rrnB T1
csgA-SpyTag
RBS
cr
pLuxR
LuxR
p15A origin
pLuxR
rrnB T
taRNA

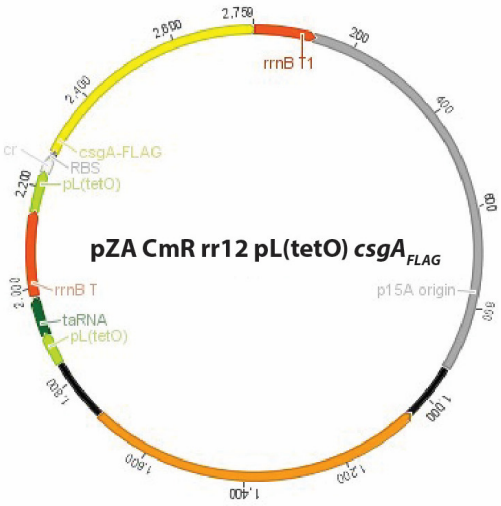
pZA CmR rr12 pL(tetO) csgA$_{FLAG}$
rrnB T1
cr
csgA-FLAG
RBS
pL(tetO)
rrnB T
taRNA
pL(tetO)
p15A origin

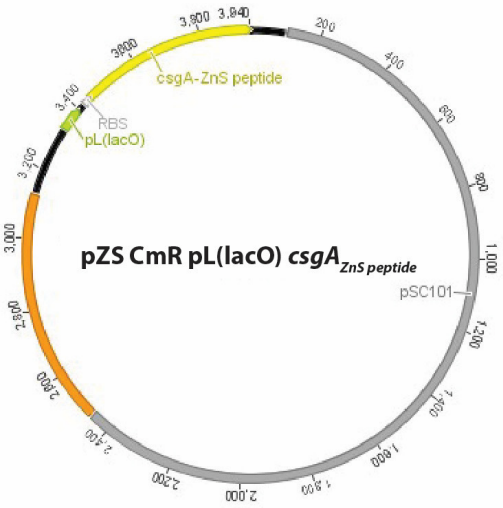
csgA-ZnS peptide
RBS
pL(lacO)
pZS CmR pL(lacO) csgA ZnS peptide
pSC101

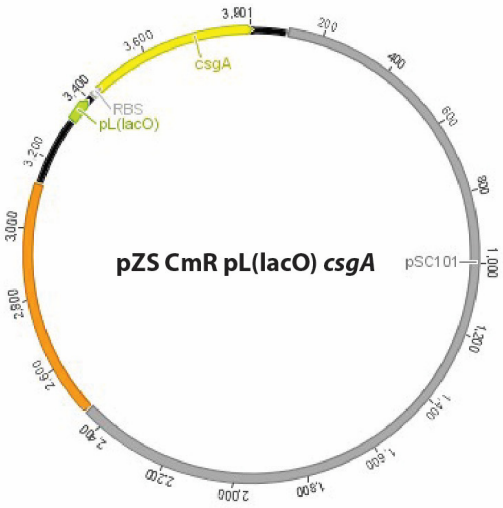
csgA
RBS
pL(lacO)
pZS CmR pL(lacO) csgA
pSC101

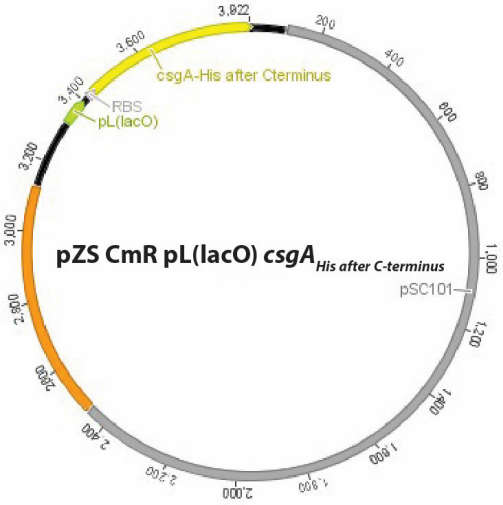
csgA-His after Cterminus
RBS
pL(lacO)
pZS CmR pL(lacO) csgA His after C-terminus
pSC101

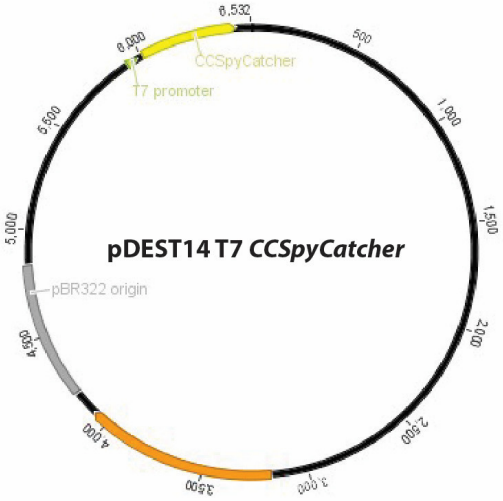
CCSpyCatcher
T7 promoter
pDEST14 T7 CCSpyCatcher
pBR322 origin

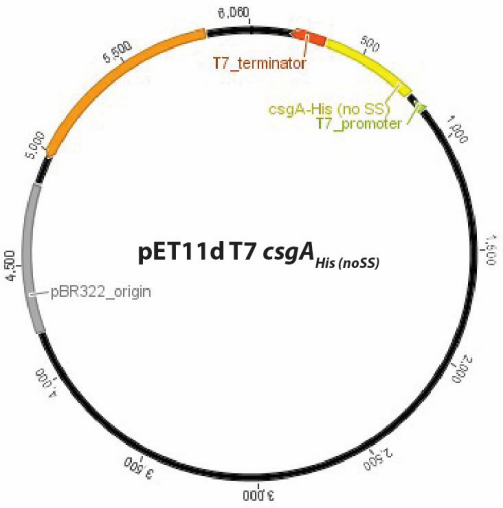
T7_terminator
csgA-His (no SS)
T7_promoter
pET11d T7 csgA His (noSS)
pBR322_origin

Supplementary Methods

Plasmid construction. The plasmids used in this study were constructed with standard molecular cloning techniques[2] using New England Biolabs (NEB) restriction endonucleases, T4 DNA Ligase, and Phusion PCR kits. A Bio-Rad S1000 Thermal Cycler with Dual 48/48 Fast Reaction Modules (Bio-Rad) was used to perform PCRs, ligations, and restriction digests. Gel extractions were carried out with QIAquick Gel Extraction Kits (Qiagen). Custom oligonucleotide primers were obtained from Integrated DNA Technologies (Coralville, IA).

All ligations for plasmid construction were transformed into *E. coli* strain DH5αPRO with standard protocols[2]. Isolated colonies were inoculated into Luria-Bertani (LB)-Miller medium (Fisher), which is LB medium with 10g/L NaCl[2], using antibiotics corresponding to antibiotic-selection markers within the plasmids (Supplementary Tables 1, 2) at the following concentrations: carbenicillin at 50μg/ml, chloramphenicol at 25μg/ml, kanamycin at 30μg/ml, and spectinomycin at 100μg/ml. DNA was extracted with Qiagen QIAprep Spin Miniprep Kits. Plasmid construct sequences were confirmed by restriction digest and sequencing was performed by Genewiz (Cambridge, MA).

The parts that constitute the plasmids used in this work are described in Supplementary Table 1, and plasmids are described in Supplementary Table 2. To create constructs for the expression of output genes under tight regulation by an aTc-inducible riboregulator, pZE-AmpR-rr12-pL(tetO)-*gfp* was used as a starting point[3]. The AmpR cassette of pZE-AmpR-rr12-pL(tetO)-*gfp* was replaced by the CmR cassette from pZS-CmR-pL(lacO)-*gfp* by using SacI-HF/AatII digestion and T4 ligation to create pZE-CmR-rr12-pL(tetO)-*gfp*. Then, the ColE1 origin of pZE-CmR-rr12-pL(tetO)-*gfp* was replaced by the p15A origin from pZA-AmpR-pL(tetO)-*gfp* by using SacI-HF/AvrII excision and T4 ligation to create pZA-CmR-rr12-pL(tetO)-*gfp*. The *gfp* gene was excised using KpnI/MluI digest to create the vector pZA-CmR-rr12-pL(tetO)-. The genes *csgA*, $csgA_{His}$, *mCherry*, and $csgA_{FLAG}$

with KpnI and MluI sticky ends were generated by PCR and KpnI/MluI digest; these fragments were ligated with pZA-CmR-rr12-pL(tetO)- to create pZA-CmR-rr12-pL(tetO)-*csgA*, pZA-CmR-rr12-pL(tetO)-$csgA_{His}$, pZA-CmR-rr12-pL(tetO)-*mCherry*, and pZA-CmR-rr12-pL(tetO)-$csgA_{FLAG}$ plasmids, respectively.

To create constructs for the expression of output genes under tight regulation by an AHL-inducible riboregulator, pZE-KanR-rr12y-pLuxR-*gfp* was used as a starting point[3]. The KanR cassette of pZE-KanR-rr12y-pLuxR-*gfp* was replaced by the CmR cassette from pZS-CmR-pL(lacO)-*gfp* by using SacI-HF/AatII digestion and T4 ligation to create pZE-CmR-rr12y-pLuxR-*gfp*. Then, the ColE1 origin of pZE-CmR-rr12y-pLuxR-*gfp* was replaced by the p15A origin from pZA-AmpR-pL(tetO)-*gfp* by using SacI-HF/AvrII excision and T4 ligation to create pZA-CmR-rr12y-pLuxR-*gfp*. The *gfp* gene was excised using KpnI/MluI digest to create the vector pZA-CmR-rr12y-pLuxR-. A codon-optimized gene encoding a CsgA variant consisting of eight tandem repeats of CsgA with a histidine tag at the C-terminus ($8XcsgA_{His}$), and flanked by KpnI and MluI sites, was designed and custom synthesized by GenScript (Piscataway, NJ). The gene $8XcsgA_{His}$ with sticky ends was generated by KpnI/MluI digest and ligated with pZA-CmR-rr12y-pLuxR- to create pZA-CmR-rr12y-pLuxR-$8XcsgA_{His}$. The genes *csgA*, $csgA_{His}$, and $csgA_{SpyTag}$, also with KpnI and MluI sticky ends, were ligated with the vector to create pZA-CmR-rr12y-pLuxR-*csgA*, pZA-CmR-rr12y-pLuxR-$csgA_{His}$, and pZA-CmR-rr12y-pLuxR-$csgA_{SpyTag}$, respectively.

A plasmid with an AmpR resistance marker was also created for use in co-culture experiments (Fig. 3). This plasmid had a low-copy origin and an output gene ($lacZ_{alpha}$) under tight repression by a riboregulator to ensure minimal effects on the host cell apart from conferring ampicillin resistance. The plasmid pZE-KanR-rr10-pL(lacO)-*mCherry* was used as a starting point[3]. The KanR cassette of pZE-KanR-rr10-pL(lacO)-*mCherry* was replaced by the AmpR cassette from pZA-AmpR-pL(tetO)-*gfp* by using SacI-HF/AatII digestion and T4 ligation to create pZE-AmpR-rr10-pL(lacO)-*mCherry*. Then, the ColE1 origin of pZE-AmpR-rr10-pL(lacO)-*mCherry* was replaced by the pSC101 origin from pZS-CmR-pL(lacO)-*gfp* by using SacI-HF/AvrII excision and T4 ligation to create pZS-AmpR-rr10-

pL(lacO)-*mCherry*. The *mCherry* gene of pZSAmpR-rr10-pL(lacO)-*mCherry* was replaced by the $lacZ_{alpha}$ gene from pZE-AmpR-pLuxR-$lacZ_{alpha}$ using KpnI/MluI excision and T4 ligation to create pZS-AmpR-rr10-pL(lacO)-$lacZ_{alpha}$.

Plasmids for expressing genes from the pL(lacO) promoter were constructed by using pZS-CmR-pL(lacO)-*gfp*[4] as a starting point. The *gfp* gene was excised by digestion with KpnI/MluI to create vector pZS-CmR-pL(lacO)-. This vector was ligated, using T4 ligase, with digested PCR fragments that had KpnI and MluI sticky ends. These fragments encoded *csgA*, $csgA_{His\ after\ C\text{-}terminus}$, or $csgA_{ZnS\ peptide}$. This created pZS-CmR-pL(lacO)-*csgA*, pZS-CmR-pL(lacO)-$csgA_{His\ after\ C\text{-}terminus}$, and pZS-CmR-pL(lacO)-$csgA_{ZnS\ peptide}$ plasmids.

The pDEST14-T7-*CCSpyCatcher* plasmid for the expression of CCSpyCatcher was created from pDEST14-T7-*SpyCatcher*[5] using the QuikChange Lightning Kit (Agilent) to add codons encoding two cysteines immediately after the start codon. The thiol groups on cysteines were used to conjugate SpyCatcher to QDs as described below.

Strain construction. To create the *E. coli* MG1655 *PRO* Δ*csgA ompR234* strain used in this study, we sequentially generated *E. coli* MG1655 *PRO* Δ*csgA::aph*, *E. coli* MG1655 *PRO* Δ*csgA*, and *E. coli* MG1655 *PRO* Δ*csgA ompR234*. The PRO cassette (P_{laci^q}/*lacI*, P_{N25}/*tetR*, $Spec^R$) has a spectinomycin resistance marker and expresses *lacI* and *tetR* at high constitutive levels[4].

E. coli MG1655 *PRO* Δ*csgA::aph* was generated via P1 transduction of the Δ*csgA::aph* mutation from donor strain JW1025-1 of the Keio collection[6] into recipient *E. coli* MG1655 *PRO*[3], as previously described[2]. To prepare P1 lysate, 100µl overnight culture of donor strain was incubated with 100µl P1 phage in 10ml LB + 7mM $CaCl_2$ + 12mM $MgSO_4$ for 20min without shaking at 37°C, then for 2h with shaking at 37°C. To produce more P1 lysate, 300µl more of donor strain was added, the culture incubated for 20min without shaking at 37°C, then for 2h with shaking at 37°C. The culture was transferred to a 50ml Falcon tube, 2ml of chloroform was added, and the mixture was vortexed and centrifuged for 15min at 3000rpm. The supernatant, containing the P1 lysate, was transferred

to Eppendorf tubes and centrifuged for 5min at 14000rpm to pellet remaining debris. For transduction, the P1 lysate was diluted 60-fold into 1ml LB + 7mM $CaCl_2$ + 12mM $MgSO_4$ in an Eppendorf tube, 100µl overnight culture of recipient strain was added, and the tube was incubated for 1h with shaking at 37°C. This culture was then plated onto LB kanamycin agar with 25mM sodium citrate to select for recipients successfully transduced with the Δ*csgA::aph* mutation. Transformants were restreaked onto LB kanamycin agar for re-isolation.

E. coli MG1655 *PRO* Δ*csgA* was generated by removing the kanamycin resistance cassette as previously described[7] (in order to free this antibiotic selection marker for subsequent usage). Briefly, MG1655 *PRO* Δ*csgA::aph* was transformed with pCP20[8] carrying the gene for FLP recombinase and selected on LB ampicillin agar at 30°C. Transformants were restreaked onto non-selective LB and grown overnight at 42°C to cure the temperature-sensitive pCP20. Isolates were patched onto LB agar containing either kanamycin or ampicillin to confirm the loss of the FRT-flanked kanamycin cassette and pCP20, respectively.

Finally, *E. coli* MG1655 *PRO* Δ*csgA ompR234* was generated via P1 transduction of the *ompR234* mutation (linked to a kanamycin resistance marker) from donor *E. coli* MG1655 *ompR234*[9] into recipient *E. coli* MG1655 *PRO* Δ*csgA* with the same protocol as above. The final strain was verified via PCR amplicon size using check primers for each locus. The *ompR234* mutation was verified via sequencing of both strands of the amplicon. We also used sequencing to verify that the *csgBAC* locus in MG1655 *PRO* Δ*csgA ompR234* perfectly matched the predicted sequence for the *csgA* knockout, with an intact *csgB* gene, as constructed in the Keio collection[6] (Supplementary Fig. 20).

Finally, cell strains used in patterning experiments in this study were created by transforming plasmids constructed above into MG1655 *PRO* Δ*csgA ompR234*, and are described in Supplementary Table 3.

Culture conditions. Seed cultures were inoculated from frozen glycerol stocks and grown in LB-Miller medium using antibiotics corresponding to the plasmids in the cells (Supplementary Table 3) at the following concentrations: carbenicillin at 50μg/ml, chloramphenicol at 25μg/ml, kanamycin at 30μg/ml, and spectinomycin at 100μg/ml. Seed cultures were grown for 12h at 37°C in 14-ml culture tubes (Falcon), with shaking at 300rpm. Experimental cultures were grown in M63 minimal medium (Amresco) supplemented with 1mM $MgSO_4$ and with 0.2% w/v glucose or 0.2% w/v glycerol (hereafter referred to as glucose-supplemented M63 or glycerol-supplemented M63, respectively); all liquid experimental cultures were grown in 24-well plate wells at 30°C with no shaking[10]. For inducing conditions, inducers used were anhydrotetracycline (Sigma) at concentrations of 1-250ng/ml and N-(β-ketocaproyl)-L-homoserine lactone (Sigma) at concentrations of 1-1000nM. All experiments reporting standard-error-of-the-mean (s.e.m.) error bars were performed in triplicate.

For experiments to show inducible biofilm formation and inducible curli production (Fig. 1; Supplementary Figs. 1, 3, 8), the following strains and growth conditions were used: $aTc_{Receiver}$/$CsgA_{His}$ at an initial seeding density of $5X10^7$ cells/ml was grown on Thermanox or polystyrene or embedded in 0.7% M63 agar, for 24h in the case of liquid media and 48h in the case of agar, with glucose or glycerol-supplemented M63, with no aTc or with 250ng/ml aTc. Positive control strain MG1655 *ompR234* and negative control strain MG1655 *PRO* Δ*csgA ompR234* were similarly cultured in M63 media, without inducer.

For experiments to show inducible biofilm formation by confocal microscopy (Fig. 1; Supplementary Figs. 2, 14), the same conditions were used as above, with the cell strains used possessing an additional constitutive mCherry-expressing plasmid, and using Thermanox coverslips. The inducible strain used was $aTc_{Receiver}$/$CsgA_{His}$ with the addition of pZE-AmpR-proB-*mCherry*, the positive control strain used was MG1655 *ompR234* / pZE-AmpR-proB-*mCherry*, and the negative control strain used was MG1655 *PRO* Δ*csgA ompR234* / pZE-AmpR-proB-*mCherry*. Cultures were grown for 4-48h.

Biofilms in flow cells (Fig. 1; Supplementary Fig. 2). PDMS (Polydimethylsiloxane; Sylgard 184; Dow Corning, MI, USA) flow devices were molded from a polystyrene master yielding a negative imprint of 4 straight channels (2mm deep/2mm wide/350mm long) and then bonded with silicone adhesive to Thermanox coverslips (Nunc). For each strain and experimental condition tested, a bacterial suspension of $5X10^7$ cells/ml in glucose or glycerol supplemented M63 was introduced into flow cells under continuous flow driven by syringe pumps (PHD Ultra, Harvard Apparatus, MA, USA) at a flow rate of 0.5µl/min. Devices were placed on an inverted Zeiss 510 Meta confocal laser-scanning microscope for the duration of the experiments. Fluorescence images were recorded across the channels at 4, 10, 24, and 48 hours using a 10x/0.45 n.a. objective. The total biomass for each experiment was calculated in ImageJ[11] for 2 dimensional surface coverage (xy) and by COMSTAT for MATLAB[12] for biofilm formation (xyz image series). For each data point, 3 z-stacks per sample were analysed across 3 samples.

Static culture biofilms (Fig. 1; Supplementary Fig. 2). Biofilm formation in static culture was quantified on Thermanox coverslips at 4 and 24 hours. Each sample was rinsed in 1XPBS to remove unattached cells, placed on a No. 1 coverslip and imaged with an inverted Zeiss 510 Meta confocal laser-scanning microscope using a 100x/1.4 n.a. oil immersion objective. Fluorescence images were recorded at multiple locations across the substrate to quantify the average biomass coverage for each substrate. Biomass was quantified as described for flow cell experiments. For each data point, 3 z-stacks per sample were analysed across 3 samples.

Transmission electron microscopy. For transmission electron microscopy (TEM), a 20µl droplet of sample was placed on parafilm (Pechiney), and a 200-mesh formvar/carbon coated nickel TEM grid (Electron Microscopy Sciences) was placed with coated side face-down on the droplet for 30-60s. In all protocols requiring incubation for greater than 10min, samples were covered with petri dish lids to minimize evaporation. The grid was then rinsed with ddH_2O by placing the grid face-down in a 30µl droplet of ddH_2O and wicking off on filter paper (Whatman), and placed face-down for 15-30s on a droplet of 2% uranyl acetate (UA)

(Electron Microscopy Sciences) filtered through 0.22µm syringe filter (Whatman). Excess uranyl acetate was wicked off and the grid was allowed to air dry. TEM images were obtained on a FEI Tecnai Spirit transmission electron microscope operated at 80kV accelerating voltage. High-resolution transmission electron microscopy (HRTEM) and energy-dispersive X-ray spectroscopy (EDS) were performed on a JEOL 2010F electron microscope operating at 200 kV.

Scanning electron microscopy. For scanning electron microscopy (SEM), biofilm samples on coverslips were coated with carbon sputtered to ~10nm with a Desk II Sputter Coater (Denton Vacuum). The samples were then imaged with a JEOL JSM-6010LA scanning electron microscope operated at 10kV accelerating voltage. Images were obtained in secondary electron imaging (SEI) mode, and elemental mapping was performed with energy-dispersive X-ray spectroscopy (EDS).

Fluorescence microscopy. Fluorescence-lifetime imaging microscopy (FLIM) was performed with a Zeiss 710 NLO multiphoton microscope with 20X objective and connected to a time-correlated single-photon counting system (Becker & Hickl). The excitation source was a 2-photon laser (Coherent Chameleon Vision II) tuned to 800nm, and emission was detected through a 590-650nm bandpass filter. FLIM decays were fit using SPCImage software (Becker and Hickl, Germany).

Lambda scan analysis of fluorescent ZnS nanocrystals was performed with a Zeiss LSM 710 NLO Laser Scanning Confocal with 10X objective and 405nm excitation laser.

Anti-CsgA immuno-labelling assay (Fig. 1, Supplementary Fig. 1). We optimized antibody concentrations and based our protocol on that used in Collinson *et al.*[13]. TEM grids (Electron Microscopy Sciences) were placed with coated side face-down on 20µl droplets of samples on parafilm for 2min. The side of the TEM grids with sample was rinsed with a 30µl droplet of ddH_2O, then placed on a 50µl droplet of Blocking Buffer (10mM Tris (pH 8.0)-0.15M NaCl-1% skim milk) for 30min, followed by transfer to a 50µl droplet of Binding Buffer (10mM Tris (pH 8.0)-0.15M NaCl-0.1% skim milk) with 1:1000 dilution of rabbit

anti-CsgA antibody (M. Chapman, University of Michigan[14,15]), where it was incubated for 1h at room temperature (RT). The grid was then rinsed four times in 50µl droplets of Wash Buffer (10mM Tris (pH 8.0)-0.15M NaCl), and subsequently transferred to a 50µl droplet of Binding Buffer with 1:10 dilution of goat anti-rabbit antibody conjugated to 10nm gold particles (Sigma), where it was incubated for 1h at RT. The grid was then rinsed four times in 50µl droplets of Wash Buffer, followed by four rinses in 30µl droplets of ddH_2O. The thoroughly washed grid was placed face-down on a droplet of filtered 2% uranyl acetate for 15-30s to negative stain the sample. Excess uranyl acetate was wicked off with filter paper and the grid was allowed to air dry. All sample preparation steps were done at RT.

NiNTA-AuNP labelling assay. For nickel nitrilotriacetic acid gold nanoparticle (NiNTA-AuNP) labelling of histidine tags displayed on CsgA, 200-mesh formvar/carbon-coated nickel TEM grids (Electron Microscopy Sciences) were placed with coated side face-down on 20µl droplets of samples on parafilm for 2min. The side of the TEM grid with sample was rinsed with a 30µl droplet of ddH_2O, then with selective binding buffer (1XPBS with 0.487M NaCl, 80mM imidazole, and 0.2v/v% Tween20), and placed face-down in a 60µl droplet of selective binding buffer with 10nM 5nm NiNTA-AuNP particles (Nanoprobes). The TEM grid and droplet on parafilm was covered with a petri dish to minimize evaporation and allowed to incubate for 90min. The grid was then washed 5 times with selective binding buffer without NiNTA-AuNP particles, then twice with 1XPBS and twice with ddH_2O. The thoroughly washed grid was placed face-down on a droplet of filtered 2% uranyl acetate for 15-30s to negative stain the sample. Excess uranyl acetate was wicked off with filter paper and grid allowed to air dry. All sample preparation steps were done at RT. Images were obtained on a FEI Tecnai Spirit transmission electron microscope operated at 80kV accelerating voltage.

AuNP binding assay. This assay was performed identically to the NiNTA-AuNP labelling assay with tannic-acid-capped 5nm AuNP (Ted Pella) in place of NiNTA-AuNP.

Verifying the specificity of the histidine-tag-NiNTA interaction (Supplementary Fig. 9). Strain $aTc_{Receiver}$/$CsgA_{His}$ was used to produce $CsgA_{His}$ fibrils and strain $aTc_{Receiver}$/CsgA was used to produce CsgA fibrils; cells were seeded at $5X10^7$ cells/ml and cultured in glucose-supplemented M63 media with 50ng/ml aTc for 24h at 30°C. $CsgA_{His}$ fibrils and CsgA fibrils were labelled with the NiNTA-AuNP labelling assay; additionally $CsgA_{His}$ fibrils were labelled with the AuNP particle binding assay.

Strain verification experiments (Supplementary Figs. 5, 8). For strain verification experiments, all cultures had an initial seeding concentration of $5X10^7$ cells/ml and were grown in M63 medium supplemented with 0.2%w/v glucose as a carbon source. For experiments to verify that the fibrils seen on TEM were self-assembled from CsgA, MG1655 *ompR234* was grown for 24h, $aTc_{Receiver}$/CsgA was grown for 14h with 62.5ng/ml aTc, and $aTc_{Receiver}$/$CsgA_{His}$ was grown for 14h with 62.5ng/ml aTc. Biofilms resulting from $aTc_{Receiver}$/CsgA and $aTc_{Receiver}$/$CsgA_{His}$ cultures were resuspended in 1XPBS and the NiNTA-AuNP particle labelling assay (above) was performed to characterize curli fibrils. For experiments to verify that insertion of histidine tags into CsgA still allows curli fibril production (Supplementary Fig. 5), $aTc_{Receiver}$/CsgA was grown for 14h with 250ng/ml aTc, $aTc_{Receiver}$/$CsgA_{His}$ was grown for 14h with 250ng/ml aTc, $AHL_{Receiver}$/CsgA was grown for 14h with 1000nM AHL, and $AHL_{Receiver}$/$CsgA_{His}$ was grown for 14h with 1000nM AHL. The resulting biofilms were resuspended in 1XPBS and TEM imaging was performed.

Experiments were performed to verify that the MG1655 *PRO* Δ*csgA ompR234* host strain does not produce curli fibrils, that $AHL_{Receiver}$/$CsgA_{His}$ only produces curli fibrils when induced by AHL, and that $aTc_{Receiver}$/$CsgA_{His}$ only produces curli fibrils when induced by aTc (Supplementary Fig. 8). MG1655 *PRO* Δ*csgA ompR234* and MG1655 *ompR234* were grown for 48h. $AHL_{Receiver}$/$CsgA_{His}$ was grown for 48h with no inducer, 1000nM AHL, or 250ng/ml aTc. Similarly, $aTc_{Receiver}$/$CsgA_{His}$ was grown for 48h with no inducer, 1000nM AHL, or 250ng/ml aTc. The resulting biofilms were resuspended in 1XPBS and TEM imaging was performed. ImageJ (NIH) was used to threshold images and calculate area covered by curli

fibrils and area covered by cells. The ratio of areas was used to quantify curli fibril production.

Crystal Violet (CV) biofilm assays (Supplementary Fig. 3). Experiments were performed to verify that $aTc_{Receiver}/CsgA_{His}$ formed thick adherent biofilms only when induced by aTc, on both Thermanox coverslips (Nunc) and on polystyrene. Thermanox coverslips were placed at the bottom of 24-well plate wells in which $aTc_{Receiver}/CsgA_{His}$, at an initial seeding density of $5X10^7$ cells/ml, was grown for 24h in glucose-supplemented M63 with no aTc or with 250ng/ml aTc, in 24-well plate wells with or without Thermanox coverslips. Positive control strain MG1655 *ompR234* and negative control strain MG1655 *PRO* Δ*csgA ompR234* were similarly cultured for 24h in glucose-supplemented M63.

Crystal violet staining and quantification was performed following a standard protocol given in O'Toole *et. al.*[16] Thermanox coverslips with biofilm were washed in ddH_2O to remove unattached cells, placed in a clean 24-well plate well with 400µl of 0.1% aqueous crystal violet (Sigma), and incubated at RT for 10-15min, after which the coverslips were washed by immersing 3-4 times in a tub of ddH_2O until no more visible dye was washed off. The Thermanox coverslips were allowed to air dry, placed back into clean 24-well plate wells, and photographs taken with a ChemiDoc MP imaging system (BioRad). For quantification of CV staining, the Thermanox coverslips were placed in 24-well plate wells and 400µl of 30% acetic acid in water was added. The coverslips were incubated for 10-15min at RT to solubilize CV. Subsequently, 125µl of solubilized CV was transferred to a 96-well plate well and absorbance at 550nm was measured, with 30% acetic acid in water as a blank.

For biofilms grown on polystyrene surface of 24-well plate wells, wash steps were performed by repeatedly immersing entire plates in a tub of ddH_2O.

Congo Red assay for quantification of curli fibril production (Supplementary Fig. 4). Cells were grown to saturation at 30°C in liquid YESCA media (10g/L casamino acids, 1g/L yeast extract) and 15µl was drop cast on YESCA agar (10g/L casamino acids, 1g/L yeast

extract, and 20g/L agar) in triplicate and grown for 72h at 30°C [17]. Colonies were scraped and resuspended in 700µl 1XPBS; 300µl of cell suspension was used for OD600 cell number normalization, and the remaining 400µl combined with 5X Congo Red (CR) for a final concentration of 20µg/ml CR, and incubated for 5min at RT. The cells and curli with bound CR were spun down at 15,000 x g for 5min, and 300µl supernatant was removed for CR quantification. Concentration of CR in supernatant was quantified by absorbance at 480nm. The amount of CR bound by cells and curli were quantified by subtracting the Ab_{480nm} of supernatant from Ab_{480nm} of 20µg/ml CR [18].

For growth of BW25113 Δ*csgA*, kanamycin at 30µg/ml was added to YESCA. For growth of BW25113 Δ*csgA* / pZS3-pL(lacO)-*csgA* and BW25113 Δ*csgA* / pZS3-pL(lacO)-$csgA_{His\ after\ C\text{-}terminus}$, chloramphenicol at 25µg/ml and kanamycin at 30µg/ml were added to YESCA.

Evaluating pL(lacO) for regulation of curli production (Supplementary Fig. 19). Cells grown to saturation at 30°C in liquid YESCA media were drop cast onto YESCA agar and grown for 48h at 30°C [17]. For growth of BW25113 Δ*csgA*, kanamycin at 30µg/ml was added to YESCA. For growth of BW25113 Δ*csgA* / pZS3-pL(lacO)-*csgA* + pZS4Int-*lacI/tetR*, chloramphenicol at 25µg/ml, spectinomycin at 100µg/ml, and kanamycin at 30µg/ml were added to YESCA. For isopropyl β-D-1-thiogalactopyranoside (IPTG) induction, 1mM IPTG was added to YESCA agar.

Patterning experiments (Figs. 2-4; Supplementary Figs. 6, 7, 10-12). In all cases, cultures were grown at 30°C with no shaking. After patterning, the resulting cell populations were resuspended in 1XPBS and the NiNTA-AuNP labelling assay and TEM imaging were performed to characterize the resulting amyloid fibrils. ImageJ (NIH) was used to measure the length of unlabelled and NiNTA-AuNP labelled fibril segments.

For tunable patterning based on changing induction time (Fig. 2a, b), $AHL_{Receiver}$/CsgA at an initial seeding density of $5X10^6$ cells/ml and $aTc_{Receiver}$/$CsgA_{His}$ at an initial seeding density of $5X10^5$ cells/ml were co-cultured in 24-well plate wells with a 12mm

glass coverslip (Ted Pella) placed at the bottom. Cells were cultured in glycerol-supplemented M63 media. The cells were first co-cultured in the presence of 50nM N-(β-ketocaproyl)-L-homoserine lactone (AHL) inducer for 18-48h. The media was then removed and the resulting cells were incubated with no-inducer media for 6h. The no-inducer media was then removed and replaced with media with 50ng/ml aTc inducer. The cells were resuspended and the cultures incubated for 16h. The resulting cells were resuspended and the NiNTA-AuNP labelling assay was performed to characterize curli fibrils. For the control experiment to produce fibrils when CsgA and $CsgA_{His}$ were secreted slowly and simultaneously without temporal separation, $AHL_{Receiver}$/CsgA and $aTc_{Receiver}$/$CsgA_{His}$ were co-cultured for 24h in glycerol-supplemented M63 media with induction by 50nM AHL and 50ng/ml aTc simultaneously.

For tunable patterning based on varying inducer concentration (Fig. 2c, d), $AHL_{Receiver}$/CsgA and $aTc_{Receiver}$/$CsgA_{His}$, each at an initial seeding density of $5X10^7$ cells/ml, were co-cultured in glucose-supplemented M63 media with AHL inducer at 0-1000nM and aTc inducer at 0-250ng/ml, for 18h.

For production of a dynamic material whose composition changes with time (Fig. 3), a cellular communication system consisting of AHL_{Sender}+$aTc_{Receiver}$/CsgA and $AHL_{Receiver}$/$CsgA_{His}$ was used. The two cell strains were co-cultured, with AHL_{Sender}+$aTc_{Receiver}$/CsgA at an initial seeding density of $5X10^6$ cells/ml and $AHL_{Receiver}$/$CsgA_{His}$ at an initial seeding density of $5X10^7$, $5X10^6$, or $5X10^5$ cells/ml. The cells were co-cultured in glucose-supplemented M63 media with 50ng/ml aTc for 4-36h. The resulting cells were resuspended and the NiNTA-AuNP labelling assay was performed to characterize curli fibrils. For controls, AHL_{Sender}+$aTc_{Receiver}$/CsgA and $AHL_{Receiver}$/$CsgA_{His}$ were grown separately. In each case, the cells were grown for 16h with 50ng/ml aTc induction, with an initial seeding density of $5X10^6$ cells/ml.

For patterning at two different length scales by combining genetic regulation of subunit expression with spatial inducer gradients (Fig. 4a, b), inducer-responsive cells were

grown in solid phase on agar with opposing AHL and aTc inducer gradients. Inducer gradient agar plates were prepared by a two-step process[19]. A 100mmX100mm square petri dish (Ted Pella) was elevated at one end by 1cm. It was first filled by 20ml of 1.5% agar glucose-supplemented M63 with 50nM AHL and was allowed to harden into an agar wedge. The plate was then laid flat and filled with 20ml of 1.5% agar glucose-supplemented M63 with 50ng/ml aTc. The plates were left for 12h to allow diffusion of inducers to set up a concentration gradient. The surface of the agar was then overlaid with 5ml of 0.7% agar glucose-supplemented M63 (top-agar) embedded with four cell strains – $AHL_{Receiver}$/CsgA, $aTc_{Receiver}$/$CsgA_{His}$, $AHL_{Receiver}$/GFP, and $aTc_{Receiver}$/mCherry – each at a cell density of $3.33X10^8$ cells/ml. The top-agar with embedded cells was allowed to harden, and the plate was incubated at 30°C for 40h. Fluorescence was imaged with a ChemiDoc MP imaging system (BioRad) and fluorescence intensity values extracted with ImageJ (NIH). Top agar was sampled and resuspended in 1XPBS, and the NiNTA-AuNP labelling assay was performed to characterize curli fibrils. For the control condition with no inducer gradients, the same procedure was carried out but the petri dish was not elevated at one end to create agar wedges.

For patterning by protein-level engineering (Fig. 4c), $AHL_{Receiver}$/8X$CsgA_{His}$ cells, at an initial seeding density of $5X10^6$ cells/ml, were cultured in glucose-supplemented M63 with 10nM AHL inducer for 28h. The resulting cells were resuspended and the NiNTA-AuNP labelling assay was performed to characterize curli fibrils. For the control experiment, $aTc_{Receiver}$/$CsgA_{His}$ at an initial seeding density of $1.5X10^6$ cells/ml was cultured in glucose-supplemented M63 with 10ng/ml aTc inducer for 28h.

For patterning at two different length scales by combining genetic regulation of subunit expression with subunit-level protein engineering (Fig. 4d), $AHL_{Receiver}$/8X$CsgA_{His}$ at an initial seeding density of $5X10^7$ cells/ml and $aTc_{Receiver}$/$CsgA_{His}$ at an initial seeding density of $5X10^5$ cells/ml were first co-cultured in glucose-supplemented M63 media with 4nM AHL inducer for 36h. The media was then removed and the resulting cells incubated with no-inducer glucose-supplemented M63 media for 6h. The no-inducer media was then

removed and replaced with glucose-supplemented M63 media with 1ng/ml aTc inducer. The cells were resuspended and the cultures were incubated for 18h.

Conductive biofilm demonstration (Fig. 5, Supplementary Figs. 13-17). To create interdigitated electrodes (IDEs) for measurement of biofilm conductance, custom shadowing masks (Tech-Etch) with holes of the appropriate dimensions (Supplementary Fig. 13) were placed over Thermanox coverslips. Gold was sputtered to a thickness of ~200nm with a Desk II Sputter Coater (Denton Vacuum) and the resulting IDEs were tested with a Keithley 4200 picoammeter with two-point probe to confirm the absence of short circuits.

IDEs were placed at the bottom of 24-well plate wells and covered with glucose-supplemented M63 media with 250ng/ml anhydrotetracycline (aTc), $aTc_{Receiver}/CsgA_{His}$ cells at $1X10^8$ cells/ml, and 100nM NiNTA-AuNP particles. The cultures were incubated at 30°C with no shaking for 24h. For control experiments, either aTc was excluded, $AHL_{Receiver}/CsgA_{His}$ cells were used in place of $aTc_{Receiver}/CsgA_{His}$ cells, or NiNTA-AuNP particles were excluded (Fig. 5, Supplementary Fig. 17). $aTc_{Receiver}/CsgA_{His}$ with the addition of pZE-AmpR-proB-*mCherry* was used to show by confocal microscopy that biofilm formation is induced by aTc in presence of 100nM NiNTA-AuNP, with images taken at 4h and 24h timepoints (Supplementary Fig. 14). Please see above for details of confocal microscopy methods.

To obtain samples of biofilms for TEM, a small amount of biofilm was scraped from the IDE substrate and resuspended in 1XPBS. IDEs were washed by repeatedly immersing in ddH_2O, laid on a flat surface, and allowed to air dry for three days. A Keithley 4200 picoammeter with two-point probe was used to carry out a voltage sweep; a voltage difference was applied across the two probes and the current measured. Resulting I-V curves were fitted to simple linear regression lines and conductance of the biofilm was obtained from the slope (Supplementary Fig. 15). SEM imaging was then performed to characterize intact biofilms; SEM imaging was performed after conductance measurements because the samples were coated with a conductive carbon layer to facilitate imaging (Fig. 5b).

Gold nanowire and nanorod synthesis (Fig. 5c). Strains $aTc_{Receiver}$/$CsgA_{His}$ and $AHL_{Receiver}$/CsgA were seeded each at a concentration of $5X10^7$ cells/ml into glucose-supplemented M63, and grown for 24h at 30°C in 24-well plates. The cells were induced with 50ng/ml aTc alone, 100nM AHL alone, or both simultaneously. The resulting cells with curli fibrils were resuspended in 1XPBS, deposited on TEM grids, and labelled with 5nm NiNTA-AuNP using the specific NiNTA-AuNP binding protocol above. Gold was specifically deposited on NiNTA-AuNP chains using the GoldEnhance™ EM kit (Nanoprobes). Gold enhancement was performed for 2min following kit instructions, resulting in gold nanowires and nanorods.

Expression and purification of SpyCatcher protein. *E. coli* BL21 DE3 pLysS / pDEST14-T7-*CCSpyCatcher* (Supplementary Table 3) was grown for 12-16h at 37°C in LB-Miller with 50µg/ml carbenicillin and 0.4mM IPTG[5]. The His-tagged SpyCatcher protein with two N-terminal cyteines was purified with Ni-NTA Spin Columns (Qiagen) following the native protein purification protocol described in the Ni-NTA Spin Kit Handbook. The buffer of the elution fraction was exchanged for 1XPBS using 0.5ml Amicon filter columns (MWCO 3kDa).

Synthesis of QDs and conjugation to SpyCatcher. CdTe/CdS QDs with a photoluminescence emission peak at 620nm were synthesized following the method described in Deng *et al.*[20]. The QDs were purified by adding isopropyl alcohol, followed by centrifugation at 15000rpm for 15min and subsequent resuspension in ddH_2O. The concentration of the CdTe/CdS QDs and the amount of additional shell precursors needed to obtain specific shell thicknesses were calculated by following the method described in Deng *et al.*: 5µl $Cd(NO_3)_2$ (as Cd^{2+} source) stock solution (25mM) and 10µl 3-mercaptopropionic acid stock solution (25mM) were combined with the CdTe/CdS QDs dispersed in 100µl ddH_2O, vortexed, and gently sonicated in a 1.5ml Eppendorf. Next, 20µl of 2mg/ml of CCSpyCatcher protein was added and gently vortexed. The pH was tuned to 12.2 by adding NaOH (1M). The reaction mixture was placed on a heating block at 90°C for 30min, and then cooled down by submerging the tube in an ice water bath. The reacted solution was loaded

into a 0.5ml Amicon filter (MWCO 30kDa, EMD Millipore), 250µl 1XPBS buffer was added to the filter, and the sample was subjected to centrifugation at 7000rpm for 5min. The washing (each wash was performed with 350µl of 1XPBS buffer) and centrifugation (7000rpm for 5min) steps were repeated three times. The final product was re-dispersed in 100µl 1XPBS. The diameter of the CdTe/CdS quantum dots was ~4nm. We measured the emission spectrum of CCSpyCatcher conjugated CdTe/CdS QDs with a NanoLog Spectrometer (HORIBA Jobin Yvon) and found an emission peak at 638nm when excited at 450nm. The particles were also visibly highly fluorescent when illuminated by a UV lamp at 365nm (Supplementary Fig. 21).

Specific binding of QD-SpyCatcher to curli fibrils (Fig. 6a). Curli fibrils deposited on TEM grids were floated on 50µl of SpyCatcher Binding Buffer (1X PBS + 350mM NaCl + 0.3v/v% Tween20) for 5min and subsequently transferred to 50µl SpyCatcher Binding Buffer with 1:333 dilution of QD-SpyCatcher, followed by incubation at RT for 45min. The grid was subsequently washed four times with 50µl droplets of SpyCatcher Binding Buffer, then washed four times with 30µl droplets of ddH_2O, followed by negative staining with UA if no subsequent AuNP binding was performed. Strain $AHL_{Receiver}$/$CsgA_{SpyTag}$ was used to produce $CsgA_{SpyTag}$ fibrils and strain $AHL_{Receiver}$/CsgA was used to produce CsgA fibrils; cells were seeded at $5X10^7$ cells/ml and cultured in glucose-supplemented M63 media with 100nM AHL for 12h at 30°C.

Specific binding of 40nm-AuNP-antibody conjugates to curli fibrils (Fig. 6a). Curli fibrils deposited on TEM grids were floated on a 50µl droplet of Blocking Buffer (10mM Tris (pH 8.0)-0.15M NaCl-1% skim milk) for 30min, followed by transfer to a 50µl droplet of Binding Buffer (10mM Tris (pH 8.0)-0.15M NaCl-0.1% skim milk) with 1:250 dilution of rabbit anti-FLAG antibody (Sigma), where it was incubated for 1h at RT. The grid was then rinsed four times in 50µl droplets of Wash Buffer (10mM Tris (pH 8.0)-0.15M NaCl), and subsequently transferred to a 50µl droplet of Binding Buffer with 1:10 dilution of goat anti-rabbit antibodies conjugated to 40nm AuNPs (Abcam), where it was incubated for 3 hours at RT. The grid was then rinsed four times in 50µl droplets of Wash Buffer, followed by four rinses

in 30µl droplets of ddH_2O and negative staining with UA. Strain $aTc_{Receiver}$/$CsgA_{FLAG}$ was used to produce $CsgA_{FLAG}$ fibrils and strain $aTc_{Receiver}$/CsgA was used to produce CsgA fibrils; cells were seeded at $5X10^7$ cells/ml and cultured in glucose-supplemented M63 media with 50ng/ml aTc for 12h at 30°C.

Co-docking of QD and AuNP to curli fibrils (Fig. 6b-c). Strains $AHL_{Receiver}$/$CsgA_{SpyTag}$ and $aTc_{Receiver}$/$CsgA_{FLAG}$ were seeded each at a concentration of $5X10^7$ cells/ml into glucose-supplemented M63 media, and grown with 12mm glass coverslips (Ted Pella) for 12h at 30°C. The cells were induced with 100nM AHL alone, 50ng/ml aTc alone, or both simultaneously. Curli was resuspended in 1XPBS, deposited on TEM grids, and the specific QD-SpyCatcher binding protocol was performed, followed by the specific AuNP-antibody binding protocol and negative staining with UA. For FLIM characterization, the QD-binding protocol followed by the AuNP-binding protocol was performed directly on rinsed coverslips with attached cells and curli fibrils, sans negative staining.

Zinc sulphide nanocrystal synthesis (Fig. 6d-e). Cells were grown for 12h in LB-Miller, washed in 1XPBS, and resuspended to a concentration of 10^{10} cells/ml. 5µl of cell suspension was drop cast on YESCA agar and grown for 30h at 30°C. For culturing BW25113 Δ*csgA* / pZS3-pL(lacO)-*csgA* and BW25113 Δ*csgA* / pZS3-pL(lacO)-$csgA_{ZnS\ peptide}$ strains, chloramphenicol at 25µg/ml was added to YESCA agar. The colony was then resuspended in 30µl ddH_2O. We used a ZnS synthesis protocol based on that given in Mao *et. al.*[21] Specifically, 10µl of cell and curli suspension was added to 1ml of 1µM $ZnCl_2$ and incubated at RT for 12h. Then, 1µM Na_2S was added, and samples were incubated at 0°C for 24h by packing in ice and placing in a 4°C room. Samples were subsequently allowed to age for 12h at RT before being deposited on TEM grids for HRTEM and glass coverslips for fluorescence characterization.

Expression and purification of mature $CsgA_{His}$noSS (Supplementary Fig. 22). For the concentration reference standard for quantitating CsgA production in biofilms by dot blot, we use purified $CsgA_{His}$noSS, which is the mature form of CsgA protein without the secretion

signal sequence that is cleaved during secretion. We followed the protocol described in Zhong *et al.*[22].

In summary, the pET11d-T7 vector (Novagen) was digested at BamHI and NcoI restriction sites, and the *csgA*$_{His}$*noSS* gene (Supplementary Table 1) was amplified by PCR with introduction of compatible overhangs for Gibson assembly. To create the pET11d-T7-*csgA*$_{His}$*noSS* plasmid (Supplementary Table 2), the digested vector and *csgA*$_{His}$*noSS* PCR product were incubated with Gibson Assembly Master Mix (NEB) at 50°C for 1h, then transformed into *E. coli* DH5α. The sequence-verified pET11d-T7-*csgA*$_{His}$*noSS* plasmid was then transformed into *E. coli* BL21 T7 Express *I*^{q} (NEB) to create the BL21 T7 Express *I*^{q} / pET11d-T7-*csgA*$_{His}$*noSS* strain (Supplementary Table 3) for protein expression.

BL21 T7 Express *I*^{q} / pET11d-T7-*csgA*$_{His}$*noSS* was grown to OD600 ~0.9 in LB-Miller containing 50μg/ml carbenicillin at 37°C. Protein expression was induced with 0.5mM IPTG at 37°C for 1h. Cells were collected by centrifugation and the pellets stored at −80°C. The cells were subsequently resuspended and lysed with Extraction Buffer (8M guanidine hydrochloride (GdnHCl), 300mM NaCl, 50mM K_2HPO_4/KH_2PO_4, pH 7.2). A total of 50ml of Extraction Buffer was used for each cell pellet from a 1.5 litre culture. Lysates were incubated at 4°C for 24h. The insoluble portions of the lysates were removed by centrifugation at 10,000 x g. 6ml of TALON cobalt resin (Clontech) was washed with Equilibration Buffer (300mM NaCl, 50mM K_2HPO_4/KH_2PO_4, pH 7.2) and the supernatant was incubated with equilibrated TALON cobalt resin for 2h at RT. Resin binding the His-tagged CsgA$_{His}$noSS was spun down, washed twice with 20ml Equilibration Buffer, and loaded into HisTALON™ Gravity Columns (Clontech). The resin was further washed with 12ml of Equilibration Buffer passed through columns. Subsequently, Wash Buffer (40mM imidazole, 300mM NaCl, 50mM K_2HPO_4/KH_2PO_4, pH 7.2) was passed through columns in 5 consecutive wash steps, using 6ml in each wash. Then Elution Buffer (300mM imidazole, 300mM NaCl, 50mM K_2HPO_4/KH_2PO_4, pH 7.2) was passed through columns to elute CsgA$_{His}$noSS in 3 consecutive elution steps, using 6ml in each elution. Fractions from wash and elution steps were then mixed with loading sample buffer (Novex 4X LDS Sample

Buffer, NuPAGE) in a 3:1 ratio and heated at 90°C for 10min. The samples were then loaded into a Novex 4-12% Bis-Tris gel (NuPAGE) and ran at 165V for 35min in MES Buffer (NuPAGE). The gel was then stained with Coomassie Blue G-250 (0.1% in 7/50/43 acetic acid/methanol/ddH_2O) by incubating at RT for 30min, followed by 3 consecutive wash steps with incubation in 25ml destaining solution (10/40/50 acetic acid/methanol/ddH_2O) for 30min at RT, followed by incubation in 25ml ddH_2O overnight at RT. The destained gel was then imaged with a Gel Doc™ XR+ System with Image Lab™ Software (Bio-rad).

Dot blot quantitation of curli production (Supplementary Fig. 22). Strains MG1655 *ompR234*, MG1655 *PRO* Δ*csgA ompR234*, and $aTc_{Receiver}$/$CsgA_{His}$ were cultured in M63 glucose at 30°C in 24-well plate wells, without shaking, for 0, 12, and 24h. $aTc_{Receiver}$/$CsgA_{His}$ cells were grown either in the presence or absence of 250ng/ml aTc. At each timepoint, culture supernatant was removed without disturbing biomass at the bottom of wells, and biomass at the bottom of wells was resuspended in 1ml ddH_2O. $CsgA_{His}$ was quantified by a standard dot blot protocol, following references in which dot blots were used to quantitate the concentrations of CsgA and other amyloid proteins[23-25]. Briefly, 2µl of samples were spotted onto Protran BA83 nitrocellulose membranes (Whatman) with a dot blot manifold (Schleicher & Schuell Minifold-I Dot-Blot System). The membrane was blocked in TBST + 5% skim milk for 30min at RT, followed by incubation in TBST + 0.1% skim milk with a 1:10000 dilution of rabbit anti-CsgA antibody (M. Chapman, University of Michigan[14,15]) for 1h at RT. The membrane was then washed three times in TBST (incubating at RT for 5min), followed by incubation in TBST + 0.1% skim milk with a 1:5000 dilution of HRP-conjugated goat anti-rabbit IgG antibody (Abcam) for 30min at RT. Subsequently, the membrane was washed three times in TBST (incubating at RT for 15min, then 2 X 5min), followed by one wash in TBS (incubating at RT for 5min). The washed membrane was incubated with SuperSignal West Pico (Thermo) chemiluminescent substrate following kit instructions, and imaged with a ChemiDoc MP imaging system (BioRad), with quantitation of spot luminescence signal intensity by Quantity One (BioRad) software. Protein concentrations were calculated from a reference curve established by serial dilutions of fibrils of purified

mature $CsgA_{His}$noSS protein, which lacks the CsgA secretion signal sequence cleaved off during secretion[26]. The purified protein was incubated at RT for ~12h to allow for fibrillization. We accounted for the difference in molecular weights between secreted $CsgA_{His}$ (15kDa) and purified $CsgA_{His}$noSS (14.2kDa), since the former has an additional His tag. The amount of $CsgA_{His}$ protein per biofilm sample grown in 24-well plate wells was divided by the 1.9cm^2 surface area of the wells to obtain μg of $CsgA_{His}$ per cm^2 of biofilm. For the 24h timepoint, for which the volume per unit area of biofilm was measured by confocal microscopy, we also calculated mg of $CsgA_{His}$ per cm^3 of biofilm.

Supplementary Tables

Supplementary Table 1 | Synthetic parts used in this work.

Part Name	Part Type	Sequence	Source
pL(tetO)	Promoter	TCCCTATCAGTGATAGAGATTGACATCCCTATCAGTGATAGAGATACTGAGCACATCAGCAGGACGCACTGACC	[4]
pLuxR *Designated "pLuxI" in* [3]	Promoter	ACCTGTAGGATCGTACAGGTTTACGCAAGAAAATGGTTTGTTATAGTCGAATA	[3]
pL(lacO)	Promoter	AATTGTGAGCGGATAACAATTGACATTGTGAGCGGATAACAAGATACTGAGCACA	[4]
P(lac)	Promoter	CCGGTTAGCGCTCTCATTAGGCACCCCAGGCTTGACACTTTATGCTTCCGGCTCGTATAATGACTGCATTTATTGGTAC	[27]
cr_rr10	Riboregulator *cis* repressor sequence	TACCTATCTGCTCTTGAATTTGGGT	[3]
cr_rr12	Riboregulator *cis* repressor sequence	TACCATTCACCTCTTGGATTTGGGT	[3]
cr_rr12y	Riboregulator *cis* repressor sequence	TACCATTCACCTCTTGGATTTAGCT	[3]
taRNA_rr10	Riboregulator *trans* activator sequence	ACCCAAATTCATGAGCAGATTGGTAGTGGTGGTTAATGAAAATTAACTTACTACTACCTTTC	[3]
taRNA_rr12	Riboregulator *trans* activator sequence	ACCCAAATCCAGGAGGTGATTGGTAGTGGTGGTTAATGAAAATTAACTTACTACTACCATATATC	[3]
taRNA_rr12y	Riboregulator *trans* activator sequence	AGCTAAATCCAGGAGGTGATTGGTAGTGGTGGTTAATGAAAATTAACTTACTACTACCATATATC	[3]
rrnB T1	Terminator	GGCATCAAATAAAACGAAAGGCTCAGTCGAAAGACTGGGCCTTTCGTTTTATCTGTTGTTTGTCGGTGAACGCTCTCCTGAGTAGGACAAATCCGCCGCCCTAGA	[3]
rrnB T	Terminator (double terminator from rrnB)	TGCCTGGCGGCAGTAGCGCGGTGGTCCCACCTGACCCCATGCCGAACTCAGAAGTGAAACGCCGTAGCGCCGATGGTAGTGTGGGGTCTCCCCATGCGAGAGTAGGGAACTGCCAGGCATCAAATAAAACGAAAGGCTCAGTCGAAAGACTGGGCCTT	[28]
luxR	Repressor	ATGAAAAACATAAATGCCGACGACACATACAGAATAATTAATAAAATTAAAGCTTGTAGAAGCAATAATGATATTAATCAATGCTTATCTGATATGACTAAAATGGTACATTGTGAATATTATTTACTCGCGATCATTTATCCTC	[3]

		ATTCTATGGTTAAATCTGATATTTCAATTCTAGATAA TTACCCTAAAAAATGGAGGCAATATTATGATGACGC TAATTTAATAAAATATGATCCTATAGTAGATTATTCT AACTCCAATCATTCACCAATTAATTGGAATATATTTG AAAACAATGCTGTAAATAAAAAATCTCCAAATGTAA TTAAAGAAGCGAAAACATCAGGTCTTATCACTGGGT TTAGTTTCCCTATTCATACGGCTAACAATGGCTTCGG AATGCTTAGTTTTGCACATTCAGAAAAAGACAACTA TATAGATAGTTTATTTTTACATGCGTGTATGAACATA CCATTAATTGTTCCTTCTCTAGTTGATAATTATCGAA AAATAAATATAGCAAATAATAAATCAAACAACGATT TAACCAAAAGAGAAAAAGAATGTTTAGCGTGGGCAT GCGAAGGAAAAAGCTCTTGGGATATTTCAAAAATAT TAGGCTGCAGTGAGCGTACTGTCACTTTCCATTTAAC CAATGCGCAAATGAAACTCAATACAACAAACCGCTG CCAAAGTATTTCTAAAGCAATTTTAACAGGAGCAAT TGATTGCCCATACTTTAAAAATTAA	
luxI	AHL signalling molecule generator	ATGACTATAATGATAAAAAAATCGGATTTTTTGGCA ATTCCATCGGAGGAGTATAAAGGTATTCTAAGTCTT CGTTATCAAGTGTTTAAGCAAAGACTTGAGTGGGAC TTAGTTGTAGAAAATAACCTTGAATCAGATGAGTAT GATAACTCAAATGCAGAATATATTTATGCTTGTGAT GATACTGAAAATGTAAGTGGATGCTGGCGTTTATTA CCTACAACAGGTGATTATATGCTGAAAAGTGTTTTTC CTGAATTGCTTGGTCAACAGAGTGCTCCCAAAGATC CTAATATAGTCGAATTAAGTCGTTTTGCTGTAGGTAA AAATAGCTCAAAGATAAATAACTCTGCTAGTGAAAT TACAATGAAACTATTTGAAGCTATATATAAACACGC TGTTAGTCAAGGTATTACAGAATATGTAACAGTAAC ATCAACAGCAATAGAGCGATTTTTAAAGCGTATTAA AGTTCCTTGTCATCGTATTGGAGACAAAGAAATTCA TGTATTAGGTGATACTAAATCGGTTGTATTGTCTATG CCTATTAATGAACAGTTTAAAAAAGCAGTCTTAAAT TAA	[27]
csgA	Curli amyloid material subunit	ATGAAACTTTTAAAAGTAGCAGCAATTGCAGCAATC GTATTCTCCGGTAGCGCTCTGGCAGGTGTTGTTCCTC AGTACGGCGGCGGCGGTAACCACGGTGGTGGCGGTA ATAATAGCGGCCCAAATTCTGAGCTGAACATTTACC AGTACGGTGGCGGTAACTCTGCACTTGCTCTGCAAA CTGATGCCCGTAACTCTGACTTGACTATTACCCAGCA TGGCGGCGGTAATGGTGCAGATGTTGGTCAGGGCTC AGATGACAGCTCAATCGATCTGACCCAACGTGGCTT CGGTAACAGCGCTACTCTTGATCAGTGGAACGGCAA AAATTCTGAAATGACGGTTAAACAGTTCGGTGGTGG CAACGGTGCTGCAGTTGACCAGACTGCATCTAACTC CTCCGTCAACGTGACTCAGGTTGGCTTTGGTAACAA CGCGACCGCTCATCAGTACTAA	[1]
csgA$_{His}$	Curli amyloid material subunit	ATGAAACTTTTAAAAGTAGCAGCAATTGCAGCAATC GTATTCTCCGGTAGCGCTCTGGCAGGTGTTGTTCCTC AGTACGGCGGCGGCGGTAACCACGGTGGTGGCGGTA ATAATAGCGGCCCAAATCACCATCACCATCACCACC ATTCTGAGCTGAACATTTACCAGTACGGTGGCGGTA ACTCTGCACTTGCTCTGCAAACTGATGCCCGTAACTC TGACTTGACTATTACCCAGCATGGCGGCGGTAATGG TGCAGATGTTGGTCAGGGCTCAGATGACAGCTCAAT CGATCTGACCCAACGTGGCTTCGGTAACAGCGCTAC TCTTGATCAGTGGAACGGCAAAAATTCTGAAATGAC	This work

		GGTTAAACAGTTCGGTGGTGGCAACGGTGCTGCAGT TGACCAGACTGCATCTAACTCCTCCGTCAACGTGACT CAGGTTGGCTTTGGTAACAACGCGACCGCTCATCAG TACCACCATCACCATCACCACCATTAA	
8XcsgA$_{His}$	Curli amyloid material subunit	ATGAAGCTGCTGAAGGTGGCTGCTATCGCTGCTATC GTGTTTTCCGGTTCGGCACTGGCTGGTGTCGTCCCGC AATACGGTGGCGGTGGCAACCATGGCGGTGGCGGTA ACAATAGTGGTCCGAACTCCGAACTGAATATTTATC AGTACGGCGGTGGCAACAGCGCACTGGCACTGCAAA CGGATGCACGTAATTCTGACCTGACCATTACGCAGC ATGGTGGCGGTAACGGCGCTGATGTGGGCCAAGGTA GTGATGACAGCTCTATCGACCTGACCCAGCGCGGCT TTGGTAATAGTGCAACGCTGGATCAATGGAACGGCA AAAATTCCGAAATGACCGTTAAGCAGTTCGGCGGTG GCAATGGTGCGGCCGTCGATCAAACCGCGTCCAACA GTTCCGTGAATGTTACGCAGGTTGGCTTTGGTAACA ATGCAACCGCTCATCAATATAACGGCAAAAATGGAT CCTCGGAACTGAACATCTATCAGTACGGTGGCGGTA ATTCAGCGCTGGCCCTGCAAACCGATGCGCGTAACT CGGATCTGACGATTACGCAGCATGGCGGTGGCAACG GTGCCGATGTCGGTCAGGGCAGCGACGATTCTAGCA TCGACCTGACGCAACGTGGCTTTGGTAACAGCGCCA CCCTGGACCAGTGGAATGGTAAAAATTCTGAAATGA CCGTGAAGCAGTTCGGTGGCGGTAATGGTGCAGCTG TTGATCAAACGGCAAGCAACAGTTCCGTCAATGTGA CCCAAGTGGGCTTCGGTAACAATGCAACGGCTCATC AATACAATGGTAAGAACGGATCCTCGGAACTGAACA TTTACCAATACGGCGGTGGCAATAGTGCCCTGGCGC TGCAAACCGATGCACGTAACTCCGATCTGACGATCA CGCAGCACGGTGGCGGTAACGGTGCTGATGTTGGCC AAGGTTCAGACGATTCTTCCATTGATCTGACGCAAC GCGGCTTTGGTAACTCAGCGACCCTGGACCAATGGA ATGGTAAGAACTCGGAAATGACCGTCAAACAATTTG GCGGTGGCAACGGGGCGGCCGTGGATCAAACCGCCT CTAACAGTTCCGTTAATGTCACGCAAGTGGGTTTCG GCAATAACGCCACGGCCCACCAGTACAATGGTAAGA ATGGATCCAGCGAACTGAATATCTACCAATATGGTG GCGGTAATAGCGCCCTGGCTCTGCAGACGGATGCGC GTAACAGCGATCTGACCATCACCCAGCACGGCGGTG GCAACGGCGCAGACGTGGGTCAGGGCAGCGATGATT CTTCTATCGACCTGACGCAGCGTGGTTTTGGTAACAG TGCAACCCTGGATCAGTGGAATGGCAAGAACAGCGA AATGACGGTTAAACAATTTGGTGGCGGTAACGGGGC AGCTGTCGATCAAACGGCCAGTAATAGTTCCGTGAA CGTGACGCAAGTTGGTTTTGGCAATAACGCGACCGC CCATCAATACAATGGCAAGAACGGATCCAGCGAACT GAACATTTATCAATATGGCGGTGGCAACTCTGCCCT GGCTCTGCAAACGGACGCCCGTAACTCGGACCTGAC GATCACCCAACATGGTGGCGGTAATGGTGCCGACGT TGGCCAAGGTAGCGACGATTCCAGCATTGATCTGAC CCAACGTGGTTTCGGTAACAGCGCGACCCTGGATCA ATGGAATGGCAAGAATAGCGAAATGACGGTCAAAC AATTCGGCGGTGGCAACGGAGCGGCCGTTGATCAAA CCGCCAGTAACAGTTCCGTCAACGTGACGCAAGTGG GTTTTGGCAATAATGCCACGGCCCACCAATACAATG GTAAAAACGGATCCTCTGAACTGAATATTTACCAGT ATGGTGGCGGTAACAGTGCCCTGGCACTGCAGACGG ACGCGCGTAACTCCGACCTGACGATCACGCAACATG GCGGTGGCAATGGCGCCGATGTTGGCCAGGGTAGCG	This work

		ACGATAGTAGCATTGATTTAACCCAGCGTGGTTTCG GCAATAGCGCCACGCTGGATCAGTGGAACGGTAAGA ATTCAGAAATGACGGTCAAGCAATTTGGTGGCGGTA ATGGGGCAGCTGTGGATCAGACGGCCAGCAATAGTT CCGTTAACGTCACCCAAGTGGGTTTCGGTAACAACG CCACGGCTCATCAGTACAATGGTAAAAATGGATCCT CCGAGTTAAACATCTACCAGTATGGCGGTGGCAATT CTGCCCTGGCCCTGCAAACGGACGCGCGCAATAGCG ATCTGACCATTACCCAACACGGTGGCGGTAATGGCG CCGACGTGGGCCAGGGTAGCGATGATAGTTCCATTG ACCTGACGCAACGCGGTTTCGGCAACAGTGCGACGC TGGACCAATGGAACGGTAAGAACTCTGAAATGACGG TGAAACAGTTTGGCGGTGGCAATGGGGCGGCCGTCG ATCAGACCGCGTCTAACAGTTCCGTGAACGTGACAC AGGTCGGTTTCGGCAATAATGCCACCGCCCATCAGT ACAATGGCAAGAATGGATCCCAATACGGTGGCGGTA ACTCGGCACTGGCACTGCAGACCGATGCACGTAATA GCGACCTGACGATTACCCAACACGGCGGTGGCAATG GAGCAGATGTGGGCCAGGGTTCTGATGACTCATCGA TTGATCTGACGCAGCGTGGCTTCGGTAATTCAGCCA CGCTGGACCAGTGGAACGGTAAAAACAGCGAGATG ACCGTTAAGCAATTCGGTGGCGGTAACGGAGCAGCT GTTGATCAGACGGCGAGCAACAGCTCTGTCAATGTG ACCCAGGTCGGTTTCGGTAATAATGCTACGGCACAT CAGTATCACCACCACCATCATCATCACTAA	
gfp	Fluorescent reporter	ATGAGTAAAGGAGAAGAACTTTTCACTGGAGTTGTC CCAATTCTTGTTGAATTAGATGGTGATGTTAATGGGC ACAAATTTTCTGTCAGTGGAGAGGGTGAAGGTGATG CAACATACGGAAAACTTACCCTTAAATTTATTTGCAC TACTGGAAAACTACCTGTTCCATGGCCAACACTTGTC ACTACTTTCGGTTATGGTGTTCAATGCTTTGCGAGAT ACCCAGATCATATGAAACAGCATGACTTTTTCAAGA GTGCCATGCCCGAAGGTTATGTACAGGAAAGAACTA TATTTTTCAAAGATGACGGGAACTACAAGACACGTG CTGAAGTCAAGTTTGAAGGTGATACCCTTGTTAATA GAATCGAGTTAAAAGGTATTGATTTTAAAGAAGATG GAAACATTCTTGGACACAAATTGGAATACAACTATA ACTCACACAATGTATACATCATGGCAGACAAACAAA AGAATGGAATCAAAGTTAACTTCAAAATTAGACACA ACATTGAAGATGGAAGCGTTCAACTAGCAGACCATT ATCAACAAAATACTCCAATTGGCGATGGCCCTGTCC TTTTACCAGACAACCATTACCTGTCCACACAATCTGC CCTTTCGAAAGATCCCAACGAAAAGAGAGACCACAT GGTCCTTCTTGAGTTTGTAACAGCTGCTGGGATTACA CATGGCATGGATGAACTATACAAATAA	[3]
mCherry	Fluorescent reporter	ATGGTGAGCAAGGGCGAAGAAGATAACATGGCCAT CATCAAGGAGTTCATGCGCTTCAAGGTGCACATGGA GGGCTCCGTGAACGGCCACGAGTTCGAGATCGAGGG CGAGGGCGAGGGCCGCCCCTACGAGGGCACCCAGA CCGCCAAGCTGAAGGTGACCAAGGGTGGCCCCCTGC CCTTCGCCTGGGACATCCTGTCCCCTCAGTTCATGTA CGGCTCCAAGGCCTACGTGAAGCACCCCGCCGACAT CCCCGACTACTTGAAGCTGTCCTTCCCCGAGGGCTTC AAGTGGGAGCGCGTGATGAACTTCGAGGACGGCGG CGTGGTGACCGTGACCCAGGACTCCTCCCTGCAGGA CGGCGAGTTCATCTACAAGGTGAAGCTGCGCGGCAC CAACTTCCCCTCCGACGGCCCCGTAATGCAGAAGAA GACCATGGGCTGGGAGGCCTCCTCCGAGCGGATGTA	[3]

		CCCCGAGGACGGCGCCCTGAAGGGCGAGATCAAGC AGAGGCTGAAGCTGAAGGACGGCGGCCACTACGAC GCTGAGGTCAAGACCACCTACAAGGCCAAGAAGCCC GTGCAGCTGCCCGGCGCCTACAACGTCAACATCAAG TTGGACATCACCTCCCACAACGAGGACTACACCATC GTGGAACAGTACGAACGCGCCGAGGGCCGCCACTCC ACCGGCGGCATGGACGAGCTGTACAAGTAA	
csgA$_{SpyTag}$	Curli amyloid material subunit	ATGAAACTTTTAAAAGTAGCAGCAATTGCAGCAATC GTATTCTCCGGTAGCGCTCTGGCAGGTGTTGTTCCTC AGTACGGCGGCGGCGGTAACCACGGTGGTGGCGGTA ATAATAGCGGCCCAAATTCTGAGCTGAACATTTACC AGTACGGTGGCGGTAACTCTGCACTTGCTCTGCAAA CTGATGCCCGTAACTCTGACTTGACTATTACCCAGCA TGGCGGCGGTAATGGTGCAGATGTTGGTCAGGGCTC AGATGACAGCTCAATCGATCTGACCCAACGTGGCTT CGGTAACAGCGCTACTCTTGATCAGTGGAACGGCAA AAATTCTGAAATGACGGTTAAACAGTTCGGTGGTGG CAACGGTGCTGCAGTTGACCAGACTGCATCTAACTC CTCCGTCAACGTGACTCAGGTTGGCTTTGGTAACAA CGCGACCGCTCATCAGTACGGCGGGGGCTCCGGCGG GGGCTCCGCGCACATCGTTATGGTCGATGCATATAA ACCCACCAAATAA	This work
csgA$_{FLAG}$	Curli amyloid material subunit	ATGAAACTTTTAAAAGTAGCAGCAATTGCAGCAATC GTATTCTCCGGTAGCGCTCTGGCAGGTGTTGTTCCTC AGTACGGCGGCGGCGGTAACCACGGTGGTGGCGGTA ATAATAGCGGCCCAAATTCTGAGCTGAACATTTACC AGTACGGTGGCGGTAACTCTGCACTTGCTCTGCAAA CTGATGCCCGTAACTCTGACTTGACTATTACCCAGCA TGGCGGCGGTAATGGTGCAGATGTTGGTCAGGGCTC AGATGACAGCTCAATCGATCTGACCCAACGTGGCTT CGGTAACAGCGCTACTCTTGATCAGTGGAACGGCAA AAATTCTGAAATGACGGTTAAACAGTTCGGTGGTGG CAACGGTGCTGCAGTTGACCAGACTGCATCTAACTC CTCCGTCAACGTGACTCAGGTTGGCTTTGGTAACAA CGCGACCGCTCATCAGTACGATTACAAGGATGACGA TGACAAGTAA	This work
csgA$_{ZnS\ peptide}$	Curli amyloid material subunit	ATGAAACTTTTAAAAGTAGCAGCAATTGCAGCAATC GTATTCTCCGGTAGCGCTCTGGCAGGTGTTGTTCCTC AGTACGGCGGCGGCGGTAACCACGGTGGTGGCGGTA ATAATAGCGGCCCAAATTCTGAGCTGAACATTTACC AGTACGGTGGCGGTAACTCTGCACTTGCTCTGCAAA CTGATGCCCGTAACTCTGACTTGACTATTACCCAGCA TGGCGGCGGTAATGGTGCAGATGTTGGTCAGGGCTC AGATGACAGCTCAATCGATCTGACCCAACGTGGCTT CGGTAACAGCGCTACTCTTGATCAGTGGAACGGCAA AAATTCTGAAATGACGGTTAAACAGTTCGGTGGTGG CAACGGTGCTGCAGTTGACCAGACTGCATCTAACTC CTCCGTCAACGTGACTCAGGTTGGCTTTGGTAACAA CGCGACCGCTCATCAGTACGGTGGTGGTTCTTGCAA CAACCCGATGCACCAGAACTGCTAA	This work

csgA$_{His\ after\ C\text{-}terminus}$	Curli amyloid material subunit	ATGAAACTTTTAAAAGTAGCAGCAATTGCAGCAATC GTATTCTCCGGTAGCGCTCTGGCAGGTGTTGTTCCTC AGTACGGCGGCGGCGGTAACCACGGTGGTGGCGGTA ATAATAGCGGCCCAAATTCTGAGCTGAACATTTACC AGTACGGTGGCGGTAACTCTGCACTTGCTCTGCAAA CTGATGCCCGTAACTCTGACTTGACTATTACCCAGCA TGGCGGCGGTAATGGTGCAGATGTTGGTCAGGGCTC AGATGACAGCTCAATCGATCTGACCCAACGTGGCTT CGGTAACAGCGCTACTCTTGATCAGTGGAACGGCAA AAATTCTGAAATGACGGTTAAACAGTTCGGTGGTGG CAACGGTGCTGCAGTTGACCAGACTGCATCTAACTC CTCCGTCAACGTGACTCAGGTTGGCTTTGGTAACAA CGCGACCGCTCATCAGTACCACCATCACCATCACCA CCATTAA	This work
CCSpyCatcher	Gene encoding the SpyCatcher protein with two N-terminal cysteines for conjugation to CdTe/CdS QDs	ATGTGTTGTTCGTACTACCATCACCATCACCATCACG ATTACGACATCCCAACGACCGAAAACCTGTATTTTC AGGGCGCCATGGTTGATACCTTATCAGGTTTATCAA GTGAGCAAGGTCAGTCCGGTGATATGACAATTGAAG AAGATAGTGCTACCCATATTAAATTCTCAAAACGTG ATGAGGACGGCAAAGAGTTAGCTGGTGCAACTATGG AGTTGCGTGATTCATCTGGTAAAACTATTAGTACATG GATTTCAGATGGACAAGTGAAAGATTTCTACCTGTA TCCAGGAAAATATACATTTGTCGAAACCGCAGCACC AGACGGTTATGAGGTAGCAACTGCTATTACCTTTAC AGTTAATGAGCAAGGTCAGGTTACTGTAAATGGCAA AGCAACTAAAGGTGACGCTCATATTTAA	[5]
csgA$_{His}$*noSS*	Gene encoding the mature form of CsgA protein without the secretion signal, with a His tag at C-terminus; purified as a reference standard for quantitating CsgA production in biofilms via dot blot	ATGGGTGTTGTTCCTCAGTACGGCGGCGGCGGTAAC CACGGTGGTGGCGGTAATAATAGCGGCCCAAATTCT GAGCTGAACATTTACCAGTACGGTGGCGGTAACTCT GCACTTGCTCTGCAAACTGATGCCCGTAACTCTGACT TGACTATTACCCAGCATGGCGGCGGTAATGGTGCAG ATGTTGGTCAGGGCTCAGATGACAGCTCAATCGATC TGACCCAACGTGGCTTCGGTAACAGCGCTACTCTTG ATCAGTGGAACGGCAAAAATTCTGAAATGACGGTTA AACAGTTCGGTGGTGGCAACGGTGCTGCAGTTGACC AGACTGCATCTAACTCCTCCGTCAACGTGACTCAGG TTGGCTTTGGTAACAACGCGACCGCTCATCAGTACC ATCACCATCACCATCACCACTAA	[22]
ampR	AmpR	ATGAGTATTCAACATTTCCGTGTCGCCCTTATTCCCT TTTTTGCGGCATTTTGCCTTCCTGTTTTTGCTCACCCA GAAACGCTGGTGAAAGTAAAAGATGCTGAAGATCA GTTGGGTGCACGAGTGGGTTACATCGAACTGGATCT CAACAGCGGTAAGATCCTTGAGAGTTTTCGCCCCGA AGAACGTTTTCCAATGATGAGCACTTTTAAAGTTCTG CTATGTGGCGCGGTATTATCCCGTATTGACGCCGGG CAAGAGCAACTCGGTCGCCGCATACACTATTCTCAG AATGACTTGGTTGAGTACTCACCAGTCACAGAAAAG CATCTTACGGATGGCATGACAGTAAGAGAATTATGC AGTGCTGCCATAACCATGAGTGATAACACTGCGGCC AACTTACTTCTGACAACGATCGGAGGACCGAAGGAG CTAACCGCTTTTTTGCACAACATGGGGGATCATGTA ACTCGCCTTGATCGTTGGGAACCGGAGCTGAATGAA GCCATACCAAACGACGAGCGTGACACCACGATGCCT GTAGCAATGGCAACAACGTTGCGCAAACTATTAACT GGCGAACTACTTACTCTAGCTTCCCGGCAACAATTA	[4]

		ATAGACTGGATGGAGGCGGATAAAGTTGCAGGACC ACTTCTGCGCTCGGCCCTTCCGGCTGGCTGGTTTATT GCTGATAAATCTGGAGCCGGTGAGCGTGGGTCTCGC GGTATCATTGCAGCACTGGGGCCAGATGGTAAGCCC TCCCGTATCGTAGTTATCTACACGACGGGGAGTCAG GCAACTATGGATGAACGAAATAGACAGATCGCTGAG ATAGGTGCCTCACTGATTAAGCATTGGTAA	
cmR	CmR	ATGGAGAAAAAAATCACTGGATATACCACCGTTGAT ATATCCCAATGGCATCGTAAAGAACATTTTGAGGCA TTTCAGTCAGTTGCTCAATGTACCTATAACCAGACCG TTCAGCTGGATATTACGGCCTTTTTAAAGACCGTAAA GAAAAATAAGCACAAGTTTTATCCGGCCTTTATTCA CATTCTTGCCCGCCTGATGAATGCTCATCCGGAATTC CGTATGGCAATGAAAGACGGTGAGCTGGTGATATGG GATAGTGTTCACCCTTGTTACACCGTTTTCCATGAGC AAACTGAAACGTTTTCATCGCTCTGGAGTGAATACC ACGACGATTTCCGGCAGTTTCTACACATATATTCGCA AGATGTGGCGTGTTACGGTGAAAACCTGGCCTATTT CCCTAAAGGGTTTATTGAGAATATGTTTTTCGTCTCA GCCAATCCCTGGGTGAGTTTCACCAGTTTTGATTTAA ACGTGGCCAATATGGACAACTTCTTCGCCCCCGTTTT CACCATGGGCAAATATTATACGCAAGGCGACAAGGT GCTGATGCCGCTGGCGATTCAGGTTCATCATGCCGTC TGTGATGGCTTCCATGTCGGCAGAATGCTTAATGAA TTACAACAGTACTGCGATGAGTGGCAGGGCGGGGCG TAA	[4]
kanR	KanR	CTCGAACCCCAGAGTCCCGCTCAGAAGAACTCGTCA AGAAGGCGATAGAAGGCGATGCGCTGCGAATCGGG AGCGGCGATACCGTAAAGCACGAGGAAGCGGTCAG CCCATTCGCCGCCAAGCTCTTCAGCAATATCACGGG TAGCCAACGCTATGTCCTGATAGCGGTCCGCCACAC CCAGCCGGCCACAGTCGATGAATCCAGAAAAGCGGC CATTTTCCACCATGATATTCGGCAAGCAGGCATCGC CATGGGTCACGACGAGATCCTCGCCGTCGGGCATGC GCGCCTTGAGCCTGGCGAACAGTTCGGCTGGCGCGA GCCCCTGATGCTCTTCGTCCAGATCATCCTGATCGAC AAGACCGGCTTCCATCCGAGTACGTGCTCGCTCGAT GCGATGTTTCGCTTGGTGGTCGAATGGGCAGGTAGC CGGATCAAGCGTATGCAGCCGCCGCATTGCATCAGC CATGATGGATACTTTCTCGGCAGGAGCAAGGTGAGA TGACAGGAGATCCTGCCCCGGCACTTCGCCCAATAG CAGCCAGTCCCTTCCCGCTTCAGTGACAACGTCGAG CACAGCTGCGCAAGGAACGCCCGTCGTGGCCAGCCA CGATAGCCGCGCTGCCTCGTCCTGCAGTTCATTCAGG GCACCGGACAGGTCGGTCTTGACAAAAAGAACCGG GCGCCCCTGCGCTGACAGCCGGAACACGGCGGCATC AGAGCAGCCGATTGTCTGTTGTGCCCAGTCATAGCC GAATAGCCTCTCCACCCAAGCGGCCGGAGAACCTGC GTGCAATCCATCTTGTTCAATCATGCGAAACGATCCT CATCCTGTCTCTTGATCAGATCTTGATCCCCTGCGCC ATCAGATCCTTGGCGGCAAGAAAGCCATCCAGTTTA CTTTGCAGGGCTTCCCAACCTTACCAGAGGGCGCCC CAGCTGGCAATTCCG	[4]
specR	SpecR	ATGCGCTCACGCAACTGGTCCAGAACCTTGACCGAA CGCAGCGGTGGTAACGGCGCAGTGGCGGTTTTCATG GCTTGTTATGACTGTTTTTTTGGGGTACAGTCTATGC CTCGGGCATCCAAGCAGCAAGCGCGTTACGCCGTGG	[4]

		GTCGATGTTTGATGTTATGGAGCAGCAACGATGTTA CGCAGCAGGGCAGTCGCCCTAAAACAAAGTTAAACA TCATGAGGGAAGCGGTGATCGCCGAAGTATCGACTC AACTATCAGAGGTAGTTGGCGTCATCGAGCGCCATC TCGAACCGACGTTGCTGGCCGTACATTTGTACGGCTC CGCAGTGGATGGCGGCCTGAAGCCACACAGTGATAT TGATTTGCTGGTTACGGTGACCGTAAGGCTTGATGA AACAACGCGGCGAGCTTTGATCAACGACCTTTTGGA AACTTCGGCTTCCCCTGGAGAGAGCGAGATTCTCCG CGCTGTAGAAGTCACCATTGTTGTGCACGACGACAT CATTCCGTGGCGTTATCCAGCTAAGCGCGAACTGCA ATTTGGAGAATGGCAGCGCAATGACATTCTTGCAGG TATCTTCGAGCCAGCCACGATCGACATTGATCTGGCT ATCTTGCTGACAAAAGCAAGAGAACATAGCGTTGCC TTGGTAGGTCCAGCGGCGGAGGAACTCTTTGATCCG GTTCCTGAACAGGATCTATTTGAGGCGCTAAATGAA ACCTTAACGCTATGGAACTCGCCGCCCGACTGGGCT GGCGATGAGCGAAATGTAGTGCTTACGTTGTCCCGC ATTTGGTACAGCGCAGTAACCGGCAAAATCGCGCCG AAGGAGGTCGCTGCCGACTGGGCAATGGAGCGCCTG CCGGCCCAGTATCAGCCCGTCATACGTGAAGCTAGA CAGGCTTATCTTGGACAAGAAGAAGATCGCTTGGCC TCGCGCGCAGATCAGTTGGAAGAATTTGTCCACTAC GTGAAAGGCGAGATCACCAAGGTAGTCGGCAAATA A	

Supplementary Table 2 | Plasmids used in this work.

Plasmid name	Plasmid ID	Description	Source
pE-AmpR-p(lac)-*luxI* *Designated "pSND-1" in* [27]	pSND-1	ColE1 origin, Amp resistance, p(lac) promoter, *luxI* output gene	[27]
pZA-AmpR-pL(tetO)-*gfp* *Designated "pZA11G" in* [4]	pZA11G	p15A origin, Amp resistance, pL(tetO) promoter, *gfp* output gene	[4]
pZS-CmR-pL(lacO)-*gfp* *Designated "pZS32G" in* [4]	pZS32G	pSC101 origin, Cm resistance, pL(lacO) promoter, *gfp* output gene	[4]
pZE-AmpR-rr12-pL(tetO)-*gfp* *Designated "rrjt12(11)g" in* [3]	rrjt12(11)g	ColE1 origin, Amp resistance, rr12 riboregulator, pL(tetO) promoter, *gfp* output gene	[3]
pZE-KanR-rr12y-pLuxR-*gfp* *Designated "rr12y(rii)g" in* [3]	rr12y(rii)g	ColE1 origin, Kan resistance, rr12y riboregulator, pLuxR promoter, *gfp* output gene	[3]
pZE-KanR-rr10-pL(lacO)-*mCherry* *Designated "rrjc10(22)mc" in* [3]	rrjc10(22)mc	ColE1 origin, Kan resistance, rr10 riboregulator, pL(lacO) promoter, *mCherry* output gene	[3]
pZE-AmpR-pLuxR-*lacZalpha*	pAYC001	ColE1 origin, Amp resistance, pLuxR promoter, $lacZ_{alpha}$ output gene	Gift of Jacob Rubens, Lu Lab
pZA-CmR-rr12-pL(tetO)-*csgA*	pAYC002	p15A origin, Cm resistance, rr12 riboregulator, pL(tetO) promoter, *csgA* output gene	This work
pZA-CmR-rr12-pL(tetO)-$csgA_{His}$	pAYC003	p15A origin, Cm resistance, rr12 riboregulator, pL(tetO) promoter, $csgA_{His}$ output gene	This work

pZA-CmR-rr12-pL(tetO)-*mCherry*	pAYC004	p15A origin, Cm resistance, rr12 riboregulator, pL(tetO) promoter, *mCherry* output gene	This work
pZA-CmR-rr12y-pLuxR-*8XcsgA$_{His}$*	pAYC005	p15A origin, Cm resistance, rr12y riboregulator, pLuxR promoter, *8XcsgA$_{His}$* output gene	This work
pZA-CmR-rr12y-pLuxR-*csgA*	pAYC006	p15A origin, Cm resistance, rr12y riboregulator, pLuxR promoter, *csgA* output gene	This work
pZA-CmR-rr12y-pLuxR-*csgA$_{His}$*	pAYC007	p15A origin, Cm resistance, rr12y riboregulator, pLuxR promoter, *csgA$_{His}$* output gene	This work
pZA-CmR-rr12y-pLuxR-*gfp*	pAYC008	p15A origin, Cm resistance, rr12y riboregulator, pLuxR promoter, *gfp* output gene	This work
pZS-AmpR-rr10-pL(lacO)-*lacZ$_{alpha}$*	pAYC009	pSC101 origin, Cm resistance, rr12y riboregulator, pL(lacO) promoter, *lacZ$_{alpha}$* output gene	This work
pZE-AmpR-proB-*mCherry*	pAYC010	ColE1 origin, Amp resistance, proB promoter, *mCherry* output gene	Gift of Tomi Jun, Lu Lab
pZA-CmR-rr12y-pLuxR-*csgA$_{SpyTag}$*	pAYC011	p15A origin, Cm resistance, rr12y riboregulator, pLuxR promoter, *csgA$_{SpyTag}$* output gene	This work
pZA-CmR-rr12-pL(tetO)-*csgA$_{FLAG}$*	pAYC012	p15A origin, Cm resistance, rr12 riboregulator, pL(tetO) promoter, *csgA$_{FLAG}$* output gene	This work
pZS-CmR-pL(lacO)-*csgA$_{ZnS\ peptide}$*	pAYC013	pSC101 origin, Cm resistance, pL(lacO) promoter, *csgA$_{ZnS\ peptide}$* output gene	This work
pZS-CmR-pL(lacO)-*csgA*	pAYC014	pSC101 origin, Cm resistance, pL(lacO) promoter, *csgA$_{ZnS}$* output gene	This work
pZS-CmR-pL(lacO)-*csgA$_{His\ after\ C\text{-}terminus}$*	pAYC015	pSC101 origin, Cm resistance, pL(lacO) promoter, *csgA$_{His\ after\ C\text{-}terminus}$* output gene	This work
pDEST14-T7-*CCSpyCatcher*	pAYC016	pBR322 origin, Amp resistance, T7 promoter, *CCSpyCatcher* output gene	This work
pET11d-T7-c*sgA$_{His}$noSS*	pAYC017	pBR322 origin, Amp resistance, T7 promoter, *csgA$_{His}$noSS* output gene	Gift of Chao Zhong, Lu Lab
pZS4Int-*lacI/tetR*	pAYC018	pSC101 origin, PRO cassette (P_{laci^q}/*lacI*, P_{N25}/*tetR*, $Spec^R$)	Expressys

Supplementary Table 3 | Cell strains used in this work.

Strain name	Strain ID	Description	Antibiotic resistance*	Source
MG1655 *ompR234* *Referred to as "ompR234" in figures*	MG1655 *ompR234*	*E. coli* strain with *ompR234* mutation that confers ability to produce curli fibrils in liquid M63 minimal media.	Kan	[9]
BW25113 Δ*csgA::aph*	BW25113 Δ*csgA::aph*	*E. coli* strain with *csgA* knock-out achieved by replacement with kanamycin resistance cassette (*aph*).	Kan	[6]
BW25113 Δ*csgA*	fAYC001	*E. coli* strain with *csgA* knocked out	N/A	This work
BL21 DE3 pLysS	BL21 DE3 *pLysS*	*E.coli* strain for inducible protein expression	Cm	Stratagene
MG1655 *PRO* Δ*csgA ompR234* *Referred to as "ΔcsgA ompR234" in figures*	fAYC002	*E. coli* strain with constitutive high level expression of *tetR* and *lacI* from *PRO* cassette derived from pZS4Int-*lacI/tetR*, with *csgA* knocked out, and with *ompR234* mutation that confers ability to produce curli fibrils in liquid M63 minimal media.	Spec, Kan	This work
$aTc_{Receiver}/CsgA_{His}$	fAYC003	*E. coli* strain that expresses $CsgA_{His}$ under tight regulation by an anhydrotetracycline (aTc) inducer-responsive riboregulator. Made by transforming pZA-CmR-rr12-pL(tetO)-$csgA_{His}$ plasmid into MG1655 *PRO* Δ*csgA ompR234*.	Spec, Kan, Cm	This work
$AHL_{Receiver}/CsgA$	fAYC004	*E. coli* strain that expresses CsgA under tight regulation by an acyl-homoserine lactone (AHL) inducer-responsive riboregulator. Made by transforming pZA-CmR-rr12y-pLuxR-*csgA* plasmid into MG1655 *PRO* Δ*csgA ompR234*.	Spec, Kan, Cm	This work
AHL_{Sender} + $aTc_{Receiver}/CsgA$	fAYC005	*E. coli* strain that constitutively produces AHL at a low basal level and inducibly expresses CsgA under tight regulation by an aTc inducer-responsive riboregulator. Made by co-transforming pZA-CmR-rr12-pL(tetO)-*csgA* and pE-AmpR-p(lac)-*luxI* into MG1655 *PRO* Δ*csgA ompR234*.	Spec, Kan, Cm, Amp	This work
$AHL_{Receiver}/CsgA_{His}$	fAYC006	*E. coli* strain that expresses $CsgA_{His}$ under tight regulation by an AHL inducer-responsive riboregulator. Made by co-transforming pZA-CmR-rr12y-pLuxR-$csgA_{His}$ and pZS-AmpR-rr10-pL(lacO)-$lacZ_{alpha}$ into MG1655 *PRO* Δ*csgA ompR234*.	Spec, Kan, Cm, Amp	This work
$AHL_{Receiver}/8XCsgA_{His}$	fAYC007	*E. coli* strain that expresses $8XCsgA_{His}$ under tight regulation by an AHL inducer-responsive riboregulator. Made by	Spec, Kan, Cm	This work

* Kanamycin (Kan), Spectinomycin (Spec), Chloramphenicol (Cm), Ampicillin (Amp)

		transforming pZA-CmR-rr12y-pLuxR-*8XcsgA$_{His}$* into MG1655 *PRO* Δ*csgA ompR234*.		
aTc$_{Receiver}$/CsgA	fAYC008	*E. coli* strain that expresses CsgA under tight regulation by an anhydrotetracycline (aTc) inducer-responsive riboregulator. Made by transforming pZA-CmR-rr12-pL(tetO)-*csgA* plasmid into MG1655 *PRO* Δ*csgA ompR234*.	Spec, Kan, Cm	This work
aTc$_{Receiver}$/mCherry	fAYC009	*E. coli* strain that expresses mCherry under tight regulation by an anhydrotetracycline (aTc) inducer-responsive riboregulator. Made by transforming pZA-CmR-rr12-pL(tetO)-*mCherry* plasmid into MG1655 *PRO* Δ*csgA ompR234*.	Spec, Kan, Cm	This work
AHL$_{Receiver}$/GFP	fAYC010	*E. coli* strain that expresses GFP under tight regulation by an acyl-homoserine lactone (AHL) inducer-responsive riboregulator. Made by transforming pZA-CmR-rr12y-pLuxR-*gfp* plasmid into MG1655 *PRO* Δ*csgA ompR234*.	Spec, Kan, Cm	This work
mCherry+ aTc$_{Receiver}$/CsgA$_{His}$	fAYC011	*E. coli* strain that expresses CsgA$_{His}$ under tight regulation by an anhydrotetracycline (aTc) inducer-responsive riboregulator, and constitutively expresses mCherry. Made by co-transforming pZE-AmpR-proB-*mCherry* and pZA-CmR-rr12-pL(tetO)-*csgA$_{His}$* into MG1655 *PRO* Δ*csgA ompR234*.	Spec, Kan, Cm, Amp	This work
MG1655 *ompR234* / pZE-AmpR-proB-*mCherry*	fAYC012	*E. coli* strain that expresses CsgA under control of native curli operon, and constitutively expresses mCherry. Made by transforming pZE-AmpR-proB-*mCherry* plasmid into MG1655 *ompR234*.	Spec, Kan, Amp	This work
MG1655 PRO Δ*csgA ompR234* / pZE-AmpR-proB-*mCherry*	fAYC013	*E. coli* strain that constitutively expresses mCherry. Made by transforming pZE-AmpR-proB-*mCherry* plasmid into MG1655 *PRO* Δ*csgA ompR234*.	Spec, Kan, Amp	This work
AHL$_{Receiver}$/CsgA$_{SpyTag}$	fAYC014	*E. coli* strain that expresses CsgA$_{SpyTag}$ under tight regulation by an AHL inducer-responsive riboregulator. Made by transforming pZA-CmR-rr12y-pLuxR-*csgA$_{SpyTag}$* into MG1655 *PRO* Δ*csgA ompR234*.	Spec, Kan, Cm	This work
aTc$_{Receiver}$/CsgA$_{FLAG}$	fAYC015	*E. coli* strain that expresses CsgA$_{FLAG}$ under tight regulation by an anhydrotetracycline (aTc) inducer-responsive riboregulator. Made by transforming pZA-CmR-rr12-pL(tetO)-*csgA$_{FLAG}$* plasmid into MG1655 *PRO* Δ*csgA ompR234*.	Spec, Kan, Cm	This work

BL21 DE3 pLysS / pDEST14-T7-*CCSpyCatcher*	fAYC016	*E. coli* strain that expresses CCSpyCatcher when induced by IPTG. Made by transforming pDEST14-T7-*CCSpyCatcher* into BL21 DE3 pLysS.	Cm, Amp	This work
BL21 T7 Express I^q / pET11d-T7-$csgA_{His}noSS$	fAYC017	*E. coli* strain that expresses $CsgA_{His}$noSS when induced by IPTG. Made by transforming pET11d-T7-$csgA_{His}noSS$ into BL21 T7 Express I^q.	Cm, Amp	Gift of Chao Zhong, Lu Lab
BW25113 Δ*csgA* / pZS-CmR-pL(lacO)-*csgA* + pZS4Int-*lacI/tetR*	fAYC018	*E. coli* strain that expresses CsgA under control of pL(lacO) promoter, along with constitutive expression of lacI and tetR. Made by co-transforming pZS-CmR-pL(lacO)-*csgA* and pZS4Int-*lacI/tetR* into BW25113 Δ*csgA*.	Kan, Cm, Spec	This work
BW25113 Δ*csgA* / pZS-CmR-pL(lacO)-$csgA_{ZnS\ peptide}$ (also referred to as "Δ*csgA*/$CsgA_{ZnS\ peptide}$")	fAYC019	*E. coli* strain that expresses $CsgA_{ZnS\ peptide}$ under control of pL(lacO) promoter. Made by transforming pZS-CmR-pL(lacO)-$csgA_{ZnS\ peptide}$ into BW25113 Δ*csgA*.	Kan, Cm	This work
BW25113 Δ*csgA* / pZS-CmR-pL(lacO)-*csgA* (also referred to as "Δ*csgA*/CsgA")	fAYC020	*E. coli* strain that expresses CsgA under control of pL(lacO) promoter. Made by transforming pZS-CmR-pL(lacO)-*csgA* into BW25113 Δ*csgA*.	Kan, Cm	This work
BW25113 Δ*csgA* / pZS-CmR-pL(lacO)-$csgA_{His\ after\ C\text{-}terminus}$	fAYC021	*E. coli* strain that expresses $CsgA_{His\ after\ R5}$ under control of pL(lacO) promoter. Made by transforming pZS-CmR-pL(lacO)-$csgA_{His\ after\ C\text{-}terminus}$ into BW25113 Δ*csgA*.	Kan, Cm	This work

References

1 Chapman, M. R. *et al.* Role of Escherichia coli curli operons in directing amyloid fiber formation. *Science* **295**, 851-855, doi:10.1126/science.1067484295/5556/851 [pii] (2002).

2 Sambrook, J., Fritsch, E.F. & Maniatis, T. *Molecular cloning: a laboratory manual.*, (Cold Spring Laboratory Press 2, 1989).

3 Callura, J. M., Cantor, C. R. & Collins, J. J. Genetic switchboard for synthetic biology applications. *Proceedings of the National Academy of Sciences of the United States of America* **109**, 5850-5855, doi:10.1073/pnas.1203808109 (2012).

4 Lutz, R. & Bujard, H. Independent and tight regulation of transcriptional units in Escherichia coli via the LacR/O, the TetR/O and AraC/I1-I2 regulatory elements. *Nucleic Acids Res* **25**, 1203-1210, doi:gka167 [pii] (1997).

5 Zakeri, B. *et al.* Peptide tag forming a rapid covalent bond to a protein, through engineering a bacterial adhesin. *Proceedings of the National Academy of Sciences of the United States of America* **109**, E690-697, doi:10.1073/pnas.1115485109 (2012).

6 Baba, T. *et al.* Construction of Escherichia coli K-12 in-frame, single-gene knockout mutants: the Keio collection. *Mol Syst Biol* **2**, 2006 0008, doi:msb4100050 [pii]10.1038/msb4100050 (2006).

7 Datsenko, K. A. & Wanner, B. L. One-step inactivation of chromosomal genes in Escherichia coli K-12 using PCR products. *Proc Natl Acad Sci U S A* **97**, 6640-6645, doi:10.1073/pnas.120163297120163297 [pii] (2000).

8 Cherepanov, P. P. & Wackernagel, W. Gene disruption in Escherichia coli: TcR and KmR cassettes with the option of Flp-catalyzed excision of the antibiotic-resistance determinant. *Gene* **158**, 9-14 (1995).

9 Prigent-Combaret, C. *et al.* Complex regulatory network controls initial adhesion and biofilm formation in Escherichia coli via regulation of the csgD gene. *Journal of bacteriology* **183**, 7213-7223 (2001).

10 Prigent-Combaret, C. *et al.* Developmental pathway for biofilm formation in curli-producing Escherichia coli strains: role of flagella, curli and colanic acid. *Environmental microbiology* **2**, 450-464 (2000).

11 Schneider, C. A., Rasband, W. S. & Eliceiri, K. W. NIH Image to ImageJ: 25 years of image analysis. *Nature methods* **9**, 671-675 (2012).

12 Heydorn, A. *et al.* Quantification of biofilm structures by the novel computer program COMSTAT. *Microbiology* **146 (Pt 10)**, 2395-2407 (2000).

13 Collinson, S. K., Emody, L., Muller, K. H., Trust, T. J. & Kay, W. W. Purification and characterization of thin, aggregative fimbriae from Salmonella enteritidis. *Journal of bacteriology* **173**, 4773-4781 (1991).

14 Hung, C. *et al.* Escherichia coli biofilms have an organized and complex extracellular matrix structure. *mBio* **4**, e00645-00613, doi:10.1128/mBio.00645-13 (2013).

15 Wang, X., Hammer, N. D. & Chapman, M. R. The molecular basis of functional bacterial amyloid polymerization and nucleation. *The Journal of biological chemistry* **283**, 21530-21539, doi:10.1074/jbc.M800466200 (2008).

16 O'Toole, G. A. Microtiter dish biofilm formation assay. *Journal of visualized experiments : JoVE*, doi:10.3791/2437 (2011).

17 Zhou, Y., Smith, D. R., Hufnagel, D. A. & Chapman, M. R. Experimental manipulation of the microbial functional amyloid called curli. *Methods Mol Biol* **966**, 53-75, doi:10.1007/978-1-62703-245-2_4 (2013).

18 Ishiguro, E. E., Ainsworth, T., Trust, T. J. & Kay, W. W. Congo red agar, a differential medium for Aeromonas salmonicida, detects the presence of the cell surface protein array involved in virulence. *Journal of bacteriology* **164**, 1233-1237 (1985).

19 Weinberg, E. D. Double-gradient agar plates. *Science* **125**, 196 (1957).

20 Deng, Z., Chen, A. Y., Zakeri, B. & Lu, T. K. Genetically engineered amyloids mediate self-assembly of quantum dots via specific covalent interactions. *Submitted.*

21 Mao, C. *et al.* Viral assembly of oriented quantum dot nanowires. *Proceedings of the National Academy of Sciences of the United States of America* **100**, 6946-6951, doi:10.1073/pnas.0832310100 (2003).

22 Zhong, C., Gurry, T., Cheng, A., Downey, J., Stultz, C.M. & Lu, T.K. Biologically Inspired Engineering of Strong, Self-Assembling, and Multi-Functional Underwater Adhesives with Synthetic Biology. *In review*.

23 Wang, X., Smith, D. R., Jones, J. W. & Chapman, M. R. In vitro polymerization of a functional Escherichia coli amyloid protein. *The Journal of biological chemistry* **282**, 3713-3719, doi:10.1074/jbc.M609228200 (2007).

24 Romero, D., Aguilar, C., Losick, R. & Kolter, R. Amyloid fibers provide structural integrity to Bacillus subtilis biofilms. *Proceedings of the National Academy of Sciences of the United States of America* **107**, 2230-2234, doi:10.1073/pnas.0910560107 (2010).

25 Bieschke, J. *et al.* Small-molecule conversion of toxic oligomers to nontoxic beta-sheet-rich amyloid fibrils. *Nature chemical biology* **8**, 93-101, doi:10.1038/nchembio.719 (2012).

26 Robinson, L. S., Ashman, E. M., Hultgren, S. J. & Chapman, M. R. Secretion of curli fibre subunits is mediated by the outer membrane-localized CsgG protein. *Molecular microbiology* **59**, 870-881, doi:10.1111/j.1365-2958.2005.04997.x (2006).

27 Basu, S., Gerchman, Y., Collins, C. H., Arnold, F. H. & Weiss, R. A synthetic multicellular system for programmed pattern formation. *Nature* **434**, 1130-1134, doi:nature03461 [pii]10.1038/nature03461 (2005).

28 Schweizer, H. P. & Hoang, T. T. An improved system for gene replacement and xylE fusion analysis in Pseudomonas aeruginosa. *Gene* **158**, 15-22 (1995).